

Demographic back-casting reveals that subtle
dimensions of climate change have strong effects
on population viability

Kevin Czachura and Tom E.X. Miller*

Program in Ecology and Evolutionary Biology, Department of
BioSciences, Rice University, Houston, TX USA

*Corresponding author: tom.miller@rice.edu (1-713-348-4218)

Abstract

- 1 1. The effects of climate change on population viability reflect the net influ-
2 ence of potentially diverse responses of individual-level demographic pro-
3 cesses (growth, survival, regeneration) to multiple components of climate.
4 Articulating climate-demography connections can facilitate forecasts of re-
5 sponses to future climate change as well as back-casts that may reveal how
6 populations responded to historical climate change.
- 7 2. We studied climate-demography relationships in the cactus *Cyclindriopun-*
8 *tia imbricata*; previous work indicated that our focal population has high
9 abundance but a negative population growth rate, where deaths exceed
10 births, suggesting that it persists under extinction debt. We parameter-
11 ized a climate-dependent integral projection model with data from a 14-year
12 field study, then back-casted expected population growth rates since 1900
13 to test the hypothesis that recent climate change has driven this population
14 into extinction debt.
- 15 3. We found clear patterns of climate change in our central New Mexico study
16 region but, contrary to our hypothesis, *C. imbricata* has most likely bene-
17 fitted from recent climate change and is on track to reach replacement-level
18 population growth within 37 years, or sooner if climate change accelerates.
19 Furthermore, the strongest feature of climate change (a trend toward years
20 that are overall warmer and drier, captured by the first principal component
21 of inter-annual variation) was not the main driver of population responses.
22 Instead, temporal trends in population growth were dominated by more sub-

23 tle, seasonal climatic factors with relatively weak signals of recent change
24 (wetter and milder cool seasons, captured by the second and third principal
25 components).

26 4. *Synthesis*. Our results highlight the challenges of **back-casting or** forecasting
27 population dynamics under climate change, since the most apparent features
28 of climate change may not be the most important drivers of ecological re-
29 sponses. Environmentally explicit demographic models can help meet this
30 challenge, but they must consider the magnitudes of different aspects of cli-
31 mate change alongside the magnitudes of demographic responses to those
32 changes.

33 Keywords

34 Cactaceae; Climate change; Demography; Extinction debt; Integral Projection
35 Model; Long-term ecological research

36 Introduction

37 Population extinction debt is likely to increase in frequency as a fingerprint of
38 global change, including climate change (Dullinger *et al.*, 2012; Urban, 2015). Ex-
39 tinction debt is a form of transient dynamics whereby populations persist despite
40 having population growth rates that fall below replacement level ($\lambda < 1$), suggest-
41 ing a long-term trajectory toward local extinction but with potentially long time
42 lags (Hastings *et al.*, 2018; Kuussaari *et al.*, 2009). While extinction debt is often
43 studied through species richness patterns at the community level (e.g., Vellend
44 *et al.* 2006), there is recent emphasis on the underlying single-species dynamics
45 whereby populations transition from positive to negative growth rates (Lehtilä
46 *et al.*, 2016; Hylander & Ehrlén, 2013). In the absence of significant migration
47 (which can maintain populations in sink habitats), extinction debt suggests that
48 the environment was more favorable for population growth at some time in the
49 past. However, the mechanisms that cause populations to tip from positive to
50 negative growth rates are rarely known, and this information may be critical for
51 effective conservation planning (Hylander & Ehrlén, 2013).

52 Structured population models built from individual-level demographic rates
53 provide a powerful framework for studying drivers of extinction debt (Lehtilä *et al.*,
54 2016) and environment-dependent population dynamics more generally (Ehrlén &
55 Morris, 2015). By incorporating climatic factors as statistical covariates, previ-
56 ous studies have identified climatic limits of population viability and forecasted
57 responses to particular types of climate change (e.g., Adler *et al.* 2013; Maschin-
58 ski *et al.* 2006; Jenouvrier *et al.* 2014). Additionally, articulating the connec-
59 tions between environment and demography can allow for ‘back-casting’ popu-

60 lation dynamics into historical environmental regimes; while rarely done (Smith
61 *et al.*, 2005), this approach may provide valuable insight regarding when and why
62 populations fell into extinction debt.

63 Many studies of climate-demography relationships focus on single climate vari-
64 ables that are known to be a dominant component of climate change and / or
65 known to have a strong influence on the focal species (e.g., Van de Pol *et al.* 2010;
66 Iler *et al.* 2019; Jenouvrier *et al.* 2009). However, for many species, it is not always
67 apparent *a priori* which dimensions of climate are most important, and this poses
68 challenges for predicting population responses to climate change. Previous studies
69 have shown that different components of climate change may have independent
70 effects on different aspects of demography or physiology (Buckley & Kingsolver,
71 2012; Frederiksen *et al.*, 2008; Van de Pol *et al.*, 2010; Lynch *et al.*, 2014). Fur-
72 thermore, different life stages (e.g., young vs old) and different vital rate processes
73 (e.g., growth, survival, reproduction) may differ in the magnitude and even di-
74 rection of their responses to single climate drivers (Doak & Morris, 2010; Dybala
75 *et al.*, 2013; Morrison & Hik, 2007; Tenhumberg *et al.*, 2018), and single life stages
76 or vital rates may be affected by multiple drivers (Dalglish *et al.*, 2011; Williams
77 *et al.*, 2015; Frederiksen *et al.*, 2008; Sletvold *et al.*, 2013). Ultimately, the influ-
78 ence of climate on population growth depends on the sensitivities of vital rates
79 to climate drivers and the sensitivities of λ to the vital rates, integrated across the
80 life cycle (McLean *et al.*, 2016; Ådahl *et al.*, 2006). These complications, common
81 to environmentally explicit demographic studies (Ehrlén *et al.*, 2016), highlight
82 the value of leveraging long-term data to gain resolution of climate drivers and the
83 importance of accounting for demographic complexity across the life cycle.

84 We used long-term demographic data to study climate-dependent population

85 dynamics of a long-lived Chihuahuan desert cactus persisting under extinction
86 debt. Our previous work with the tree cholla cactus (*Cylindriopuntia imbricata*
87 Haw. D.C.) (Cactaceae) indicated, with >95% certainty, that our focal population
88 in the northern Chihuahuan Desert (New Mexico, USA) is in decline (stochastic
89 population growth rate $\lambda_S < 1$) despite current densities that are reasonably high
90 (Ohm & Miller, 2014; Miller *et al.*, 2009; Elderd & Miller, 2016). This region has
91 experienced strong climatic fluctuations over the past century, including several
92 decadal-scale droughts interrupted by relatively wet periods (Peters *et al.*, 2015).

93 Our study was conducted in the following steps. First, we characterized climate
94 variation and change in our northern Chihuahuan desert study region over the past
95 century. Second, we estimated vital rate responses to inter-annual climate vari-
96 ation during the demographic study period (2004–2017). We hypothesized that
97 high-sensitivity vital rates (those that strongly influence λ) would be less respon-
98 sive environmental variability than low-sensitivity vital rates (Pfister, 1998). Third,
99 we back-casted climate-dependent demography to determine whether the past cen-
100 tury included periods that were favorable for population growth, thus testing the
101 hypothesis that recent climate change has driven this population into extinction
102 debt. Our analysis relied on a Bayesian framework that incorporates key sources
103 of uncertainty into our back-cast. Finally, we asked whether the components of
104 climate that are changing most strongly in this system are the same climate com-
105 ponents that most strongly influence cactus demography.

Materials and methods

Focal species, study site, and demographic data collection

Tree cholla cactus is widely distributed throughout desert and grassland habitats of the southwest U.S. and northern Mexico. These long-lived plants (40-plus years) grow through the production and elongation of cylindrical stem segments. These vegetative structures as well as flowerbuds are initiated in late spring. Flowering occurs in early summer and stem segment elongation takes place during the remainder of the growing season. For climate analyses, we divide the calendar year into warm-season months (May through September), when stem elongation, flowering, and seed production occur, and cool-season months (October through April).

This study was conducted at the Sevilleta National Wildlife Refuge (SNWR), a Long-Term Ecological Research site (SEV-LTER) in central New Mexico and near the center of this species' geographic distribution. Our study population occurs in the Los Piños mountains at an elevation of 1790 m. Tree cholla are a dominant component of the vegetation in this area (0.1 m^{-2} : Miller *et al.* 2009), along with oaks, yucca, Piñon pine, and the grasses *Bouteloua gracilis* and *B. eriopoda*.

The present study relies on long-term (2004–2017) demographic data on individual-level measures of growth, survival, and reproduction recorded from tagged plants in the Los Piños population that were censused in late May each year. This was a pre-breeding census that corresponds to the initiation of vegetative and reproductive structures (Fig. C1). We treat May 1 as the start of the transition year (coincident with the start of the warm-season months). There were a total of 1172 unique individuals in the data set and 7442 transition-year observations from 4–8

130 plots or spatial blocks depending on the year. Full details of the study design and
131 data collection are given elsewhere (Miller *et al.*, 2009; Ohm & Miller, 2014; Elderd
132 & Miller, 2016).

133 **Climate data**

134 Our goal was to connect inter-annual variation in demography to corresponding
135 variation in temperature and precipitation. SEV-LTER collects climate data from
136 a network of meteorological stations throughout SNWR. While the SEV-LTER
137 climate data cover years of our demographic data collection, our intention was
138 to back-cast demographic performance farther back into the 20th century. We
139 therefore gathered climate data from ClimateWNA v5.60 (Wang *et al.*, 2016), a
140 software package that uses PRISM (Daly *et al.*, 2008) and WorldClim (Hijmans
141 *et al.*, 2005) data to calculate downscaled data for western North America based
142 on location and elevation, going as far back as 1900. We derived seasonal estimates
143 (warm- and cool-season) of total precipitation and mean, minimum, and maximum
144 temperature from monthly climate data, for a total of eight variables. Months were
145 aligned to correspond to demographic transition years rather than calendar years,
146 which means the cool-season climate for a transition year beginning in May of year
147 t spans October of year t through April of year $t + 1$ (Fig. C1).

148 To reduce the dimensionality of the climate data, we conducted Principal Com-
149 ponents Analysis (PCA) on the eight climate variables for the years 1900-2017,
150 with climate values scaled to unit variance. We estimated the variance in the raw
151 climate data explained by each PC and the variable loadings, which give the cor-
152 relations between original variables and PC values. PCA allowed us to rank the

153 magnitudes of multiple aspects of climate variation and change by examining how
154 warm- and cool-season variables loaded onto the ranked PC axes.

155 By relying on downscaled, interpolated climate data instead of direct observa-
156 tions from meteorological stations we are trading off local resolution in favor of
157 more historical years of data. We quantified this loss of resolution by comparing
158 predictions from ClimateWNA to SEV-LTER data for years that they over-lapped,
159 using the SEV-LTER meteorological station that was nearest our study popula-
160 tion (Appendix A). We found that the two data sets were generally well correlated
161 (Table A1, Fig. A1,A2), which bolstered our confidence in ClimateWNA for back-
162 casting demographic responses to climate over the historical record. We further
163 explored the implications of using downscaled data by repeating all of our analy-
164 ses (described next) with SEV-LTER meteorological data and comparing results
165 between the two data sources (Appendix A).

166 Statistical estimation of climate-dependence

167 We fit generalized linear mixed effects models in a hierarchical Bayesian framework
168 to quantify climate dependence in demographic vital rates, as captured by three
169 principal components of climatic variability. The choice of three PCs was based
170 on results of parallel analysis (Fig. A3), a statistical method for determining how
171 many components to retain (Franklin *et al.*, 1995). There were four vital rates
172 measured in the long-term study for which we could estimate climate dependence:
173 survival from year t to year $t+1$, individual growth (change in size from year
174 t to year $t+1$), probability of flowering in year t , and the number of flowerbuds
175 produced year in t , given that a plant flowered. Survival and growth from year $t-1$

176 to t were dependent on size in year $t - 1$, and the climate covariate corresponded
 177 to the climate year $t - 1$ to t . Reproductive status and fertility in year t were
 178 dependent on size in year t and on climate from $t - 1$ to t . This timing of size
 179 and climate effects was intended to match processes in the population model (Fig.
 180 C1). We did not quantify climate-dependence in seedling recruitment. While we
 181 searched plots each year and added newly detected plants to the census, we could
 182 not confidently assign a birth year to these new additions (seedlings require several
 183 years of growth before they are consistently detectable in our census) so we do not
 184 know the climatic conditions under which they recruited.

185 All of the models for climate-dependent vital rates used the same linear predic-
 186 tor for the expected value (μ) but applied a different link function ($f(\mu)$) depending
 187 on the distribution of the observations:

$$\begin{aligned}
 f(\mu) = & \beta_0 + \beta_1 x + \\
 & \rho_1^1 PC1 + \rho_2^1 PC1^2 + \rho_3^1 x PC1 + \\
 & \rho_1^2 PC2 + \rho_2^2 PC2^2 + \rho_3^2 x PC2 + \\
 & \rho_1^3 PC3 + \rho_2^3 PC3^2 + \rho_3^3 x PC3 + \\
 & \phi + \tau
 \end{aligned} \tag{1}$$

188 The linear predictor includes a grand mean intercept (β_0) and size-dependent
 189 slope (β_1). The size variable x is the natural logarithm of plant volume ($\log_e(cm^3)$),
 190 which was standardized to mean zero and unit variance for analysis. Other fixed-
 191 effect coefficients (ρ) correspond to climate variables and climate \times size inter-
 192 actions. We include quadratic terms for climate to account for the possibility of

193 non-monotonic climate responses. Climate coefficient (ρ) superscripts correspond
194 to each PC, and subscripts correspond to linear, quadratic, and size-interaction ef-
195 fects. Finally, the linear predictor includes normally distributed random effects for
196 plot-to-plot variation ($\phi \sim N(0, \sigma_{plot})$) and year-to-year variation that is unrelated
197 to climate effects captured by PCs 1-3 ($\tau \sim N(0, \sigma_{year})$). The year random-effect
198 can be interpreted as inter-annual variability in demography that cannot be ex-
199 plained by the climate PCs. We used stochastic variable selection in a Bayesian
200 framework to reduce model complexity, dropping coefficients that were effectively
201 zero with $\geq 90\%$ certainty. Complete methods for variable selection are provided
202 in Appendix B.

203 The growth data were normally distributed; this model applied the identity
204 link and included an additional parameter for residual variance. We explored size-
205 dependence in the residual variance of growth (which determines how individuals
206 are distributed around their expected future size) but found that this led to poorer
207 model fits, so we proceeded to assume a constant value. The survival and flower-
208 ing data were Bernoulli distributed, and these models applied the logit link func-
209 tion. The fertility data (flowerbud counts) were modeled as Poisson-distributed,
210 including an individual-level random effect to account for overdispersion. All co-
211 efficients were given vague priors. We evaluated model fits using posterior predic-
212 tive checks (Elder & Miller, 2016). All models were fit using JAGS (Plummer
213 *et al.*, 2003) and R2JAGS (Su & Yajima, 2012). Analysis code is available at
214 https://github.com/texmiller/cholla_climate_IPM.

215 Demographic modeling

216 Model description

217 The statistical models described above formed the backbone of the integral projec-
218 tion model (IPM) that we used to estimate population growth in variable climate
219 environments. Following previous studies (Compagnoni *et al.*, 2016; Ohm & Miller,
220 2014; Elderd & Miller, 2016), we modeled the life cycle of *C. imbricata* using con-
221 tinuously size-structured plants, $n(x)$, and two discrete seed banks ($B_{1,t}$ and $B_{2,t}$)
222 corresponding to 1 and 2-year old seeds:

$$B_{1,t+1} = \kappa \delta \int_L^U P(x, \mathbf{c}_{t-1}; \alpha_t^P) F(x, \mathbf{c}_{t-1}; \alpha_t^F) n(x)_t dx \quad (2)$$

$$B_{2,t+1} = (1 - \gamma_1 B_{1,t}) \quad (3)$$

223 Functions P and F give the probability of flowering and the number of flowerbuds
224 produced, respectively, for an x -sized plant. The vector \mathbf{c}_{t-1} contains the climate
225 PC values for climate-year $t - 1$, which affects flowering and fertility in year t , and
226 hence the 1-year old seed bank in year $t + 1$. Parameters α_t^P and α_t^F are random
227 year effects estimated from the statistical models. The integral is multiplied by
228 the number of seeds per fruit (κ) and probability of seed dispersal/survival (δ) to
229 give the number of seeds that enter the 1-year old seed bank. Parameters L and U
230 are the lower and upper bounds, respectively, of the plant size distribution. Plants
231 can recruit out of the 1-year old seed bank with probability γ_1 or transition to the
232 2-year old seed bank with probability $(1 - \gamma_1)$. Seeds in the 2-year old seed bank
233 are assumed to either germinate (probability γ_2) or die.

234 Continuous-size dynamics were given by:

$$n(y)_{t+1} = (\gamma_1 B_{1,t} + \gamma_2 B_{2,t}) \eta(y) \omega + \int_L^U S(x, \mathbf{c}_t; \alpha_t^S) G(y, x, \mathbf{c}_t; \alpha_t^G) n(x)_t dx \quad (4)$$

235 The first term indicates recruitment from the seed banks to size y , where $\eta(y)$
 236 gives the seedling size distribution, assumed normal with mean μ_s and standard
 237 deviation σ_s . Mortality between germination (late summer) and the yearly demo-
 238 graphic census (May) is accounted for with survival probability ω . In the second
 239 term, functions S and G give the probabilities of surviving to year $t+1$ and grow-
 240 ing to size y , respectively, for an x -sized plant in year t . Climate-dependence and
 241 random year effects are included as in Eq. 2, except the timing of climate effects
 242 is shifted such that growth and survival from t to $t+1$ are affected by climate over
 243 the same interval (Fig. C1). As above, survival and growth functions also take
 244 time-varying random intercepts. Field data used to estimate seed and seed bank
 245 parameters are described elsewhere (Compagnoni *et al.*, 2016; Elderd & Miller,
 246 2016). All parameter estimates are provided in Table C1.

247 Model analysis

248 For analysis, we discretized x into b bins, replacing the continuous kernel with an
 249 b -by- b matrix (because our model also included two additional discrete states, the
 250 final projection matrix had dimensions $b+2$ -by- $b+2$). We used $b = 200$ bins. We
 251 extended integration limits L and U to avoid unintentional “eviction” (Williams
 252 *et al.*, 2012).

253 We estimated the asymptotic population growth rate λ as the dominant eigen-

254 value of the discretized IPM kernel. We compared the observed size distribution
 255 and the predicted distribution at the long-term mean climate ($PC_1 = PC_2 =$
 256 $PC_3 = 0$) and found generally good agreement (Fig. C2). We then evaluated how
 257 λ responded to climate variation by first varying each climate PC independently,
 258 holding the other two fixed at their long-term mean. Second, we back-casted λ
 259 over the entire climatological record that we had available (1900–2017), which gen-
 260 erated a time series of λ_t . We used linear regression to test for temporal trends
 261 in λ over this period. We incorporated two types of uncertainty into back-casted
 262 values of λ : imperfect knowledge of the parameter values (“estimation error”) and
 263 year-to-year fluctuations that were not related to climate (“process error”); the
 264 latter was estimated from the variances of random year effects. For the years of
 265 demographic data collection (2004–2017), we additionally quantified the deviations
 266 between predicted λ based solely on climate and “observed” λ that reflects climate
 267 and non-climate year effects (quotations indicate that these are the asymptotic pre-
 268 dictions given the vital rates observed in that year). We also conducted a similar
 269 analysis of λ_S using a 10-year sliding window (Appendix C), and we explored the
 270 consequences of extrapolating vital rate responses to climate values more extreme
 271 than those observed during the study period (Appendix D).

Finally, we used Life Table Response Experiments (LTREs) to decompose
 which combinations of climate PCs and vital rate responses were most strongly
 responsible for temporal fluctuations in the back-casted time series λ_t . We used
 a fixed-design LTRE (Caswell, 2001) where λ_t was defined as a linear function of

climate predictors:

$$\lambda_t = \bar{\lambda} + \sum_{i=1}^3 \gamma_i PC_{i,t} \quad (5)$$

There is no error term because, in this analysis, climate PCs are assumed to be the sole drivers of fluctuations in λ_t . The coefficient for each climate PC was approximated as:

$$\gamma_i \approx \sum_{j=1}^n \frac{\partial \bar{\lambda}}{\partial \theta_j} \frac{\partial \theta_j}{\partial PC_i} \quad (6)$$

272 The LTRE approximation is based on the product of the sensitivity of λ to the vital
273 rates (θ), evaluated at the long-term mean climate ($PC_1 = PC_2 = PC_3 = 0$), and
274 the sensitivity of the vital rates to climate, summed over all vital rates. Because
275 LTRE components are additive, we summed LTRE estimates over the intercept
276 and slope of each vital rate function so that we could interpret the results in terms
277 of vital rate contributions.

278 Results

279 Climate trends

280 Three principal components cumulatively explained 73.3% of the inter-annual vari-
281 ation in climate (Figure 1A). PC1 was dominated by inter-annual differences in
282 temperature and precipitation, regardless of season, and the three components
283 of temperature (mean, min, max) loaded similarly onto this component (Figure
284 1B). Over the last century, PC1 trends have fluctuated, with prolonged stretches

285 of warm and dry years (the 1950s and early 2000s) and other periods of cool
286 and wet years (early 1900s and 1970s-80s), though the overall temporal trend for
287 PC1 was negative. The decline per-year was nearly five times stronger since 1970
288 compared to the long-term average (Fig. 1C), suggesting an accelerating trajec-
289 tory of warmer and drier years. PC2 was strongly driven by cool-season climate,
290 especially precipitation, such that greater values corresponded to wetter winters
291 with low temperature maxima and high temperature minima (Figure 1B). Warm-
292 season temperatures also loaded positively onto this axis to a lesser degree (Figure
293 1B). PC2 has increased since 1900 and the change per-year was nearly four times
294 stronger since 1970 (Figure 1D), indicating an accelerating trend of wetter cool
295 seasons with moderate winter temperatures. Lastly, PC3 was correlated with a
296 combination of warm- and cool-season climate variables. The strongest variable
297 loadings on this component were minimum and mean temperatures in the cool
298 season and warm-season precipitation. Temporal trends for PC3 showed weak de-
299 clines since 1900, corresponding to milder winters with higher minimum and mean
300 temperatures and wetter warm seasons; this trend has been slightly stronger since
301 1970 (Figure 1E).

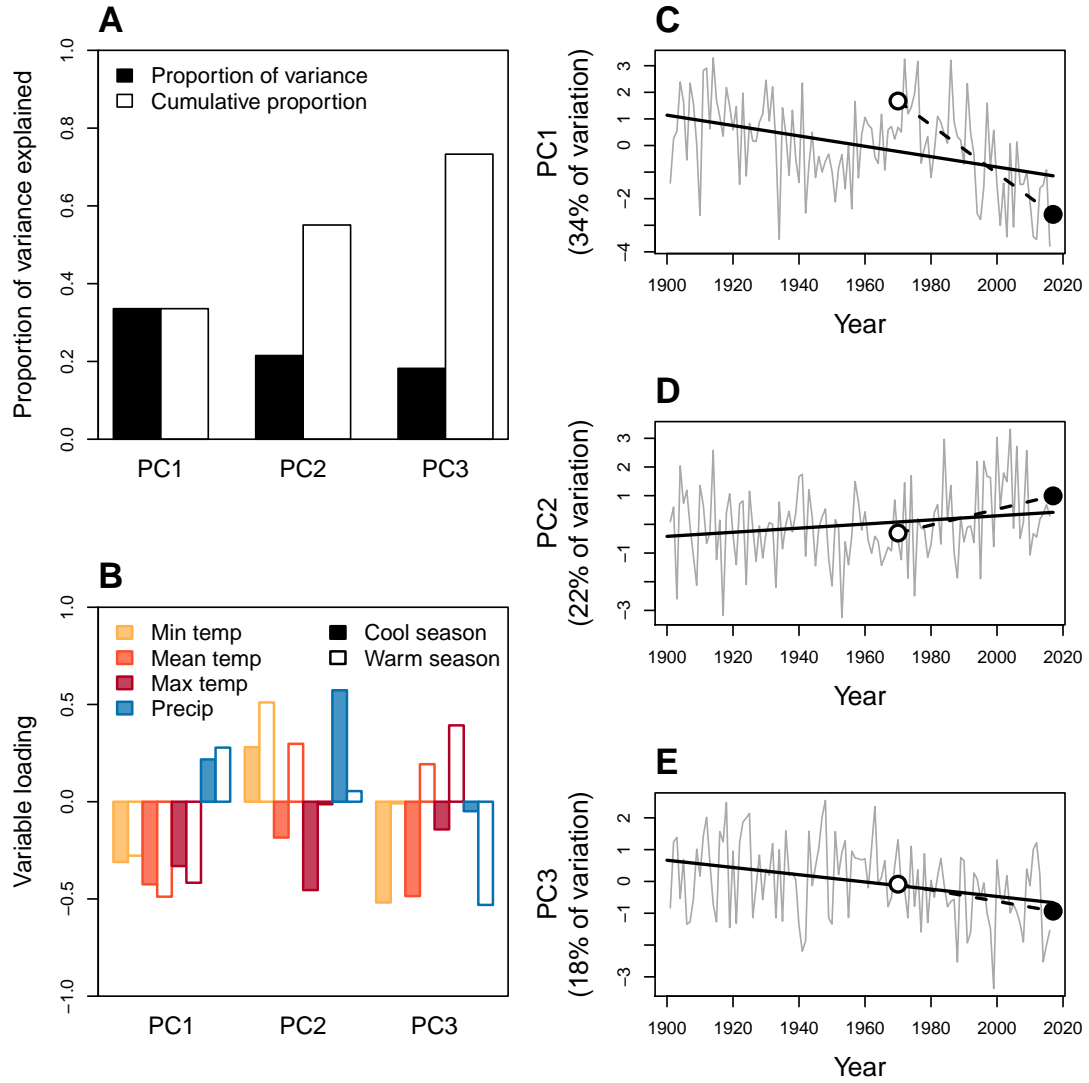


Figure 1: Principal components analysis (PCA) of inter-annual climate variability at SNWR, 1901–2017. **A**, Proportion and cumulative proportion of variation in seasonal temperatures (minimum, mean, maximum) and precipitation explained by the first three PCs. **B**, Loadings of seasonal climate variables onto PC1-3. Because climate data were standardized to mean zero and unit variance, loadings can be interpreted as the correlation between the climate variable and the PC. **C–E**, Time series of PC values, with regression lines showing long-term trends since 1901 (solid lines) or 1970 (dashed lines); open and filled points indicate the years 1970 and 2017, respectively, and correspond to the same shapes in Fig. 3

Vital rate responses to climate

Demographic vital rates estimated from long-term data (survival, growth, reproductive status, and fertility of flowering plants) were least responsive to PC1, the dominant axis of climate variability and change. All of the vital rates were strongly, positively size-dependent but there was heterogeneity in the magnitude and sign of responses to different dimensions of climate variability. Figure 2 shows vital rate data and fitted statistical models following variable selection procedures that eliminated coefficients that were weakly supported (Table B1). There was very little support for coefficients of quadratic climate effects (Table B1), indicating that responses to climate were monotonic over the range of variation we observed.

For PC1, there was a weak reduction in survival probability (especially for smaller plants; Fig. 2A) and a moderate reduction in flowering probability (especially for larger plants; Fig. 2G) at higher PC values, i.e., in cooler and wetter years. Fertility of flowering plants was not responsive to PC1 variation (Fig. 2J) and growth was not responsive to any of the climate PCs (Fig. 2D,E,F). There were positive responses to PC2 in survival (Fig. 2B), flowering probability (Fig. 2H), and fertility of flowering plants (Fig. 2K), indicating that these vital rates benefitted from years with wetter cool seasons. Responses to PC3 varied in sign, with survival increasing with decreasing PC values (years with mild winter temperature minima and wet summers) and reproductive rates increasing with increasing PC values (years with low winter minima and dry summers) (Fig. 2C,I,L).

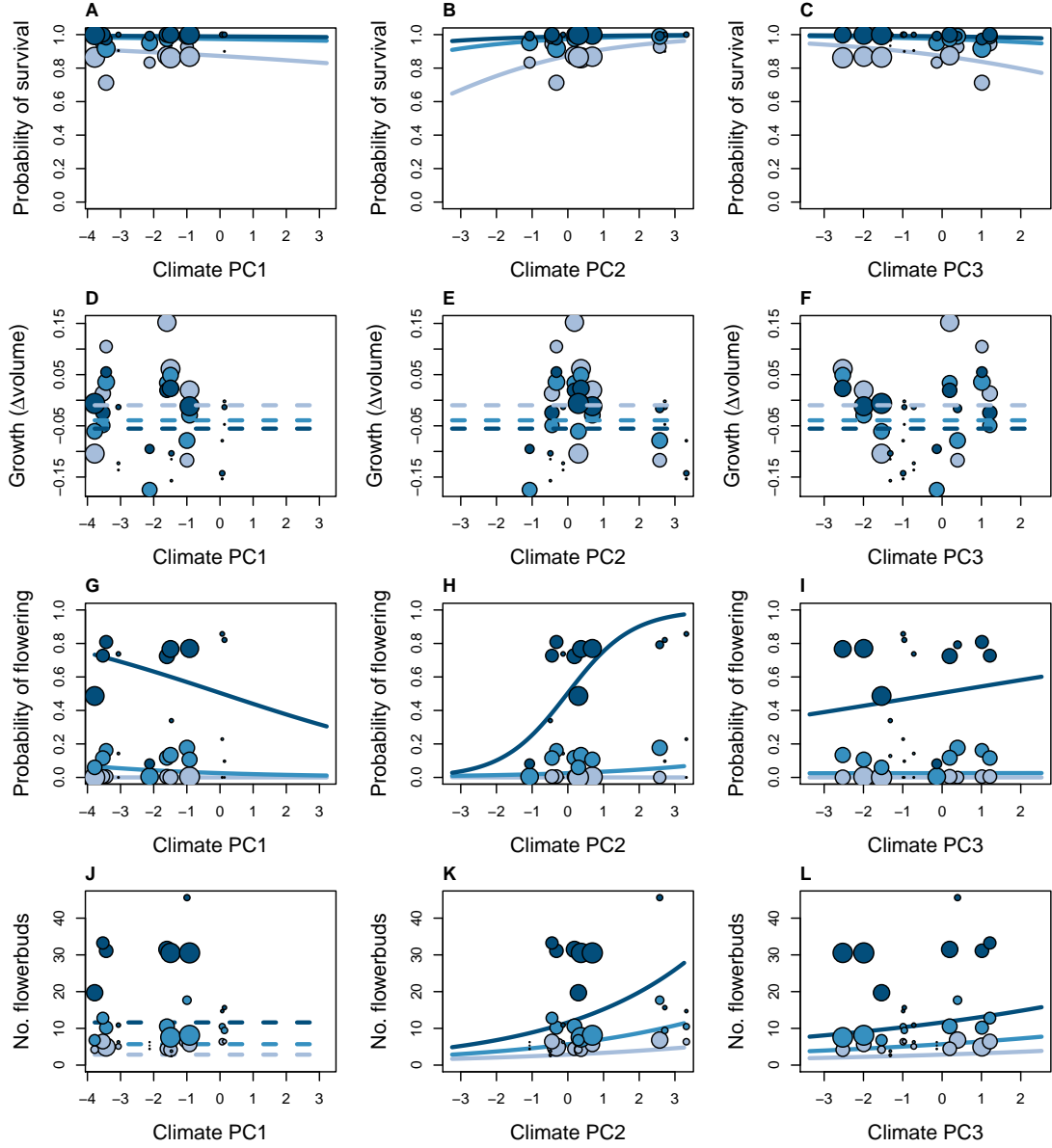


Figure 2: Climate- and size-dependent variation in survival (A-C), growth (D-F), flowering (G-I), and fertility of flowering plants (J-L) in relation to three principal components of seasonal climate variation (columns). For visualization only, the plant size distribution was discretized into three groups (small, medium, and large, corresponding to increasingly dark shading). Points show means for each size group in each year, where different years have unique PC values and point size is proportional to sample size for each size group in each year. Lines show fitted statistical models using posterior mean parameter values, with shading corresponding to size groups. Dashed lines indicate that the climate predictor was not statistically supported. Ranges of x -axes show the climate extrapolation that was required for back-casting.

Climate-dependent population growth

The population growth rate λ was predicted to increase with decreasing values of PC1 (hotter, drier years), holding other PCs fixed at their long-term average (Fig. 3A). Population growth was also predicted to increase with increasing values of PC2 (wetter cool seasons; Fig. 3B). Population growth was more sensitive to PC2 than PC1, such that the predicted change in λ from 1970 to 2017 was slightly greater for PC2 even though PC1 exhibited much greater change than PC2 over this period. Finally, greater values of PC3 (colder winters and drier summers) were predicted to cause declines in population growth, indicating that negative effects on cactus survival outweighed positive effects of PC3 on reproduction (Fig. 2). PC3 has changed relatively little since 1970 but this was associated with a change in λ of about half the magnitude to the response to relatively large change in PC1. Overall, recent climate change in each of the principal components, in isolation, has been in the direction that favors increased population growth (Fig. 1, 3). However, mean estimates for population growth rates were consistently below replacement level for all climate PC values, and the posterior probability densities rarely met or exceeded $\lambda = 1$.

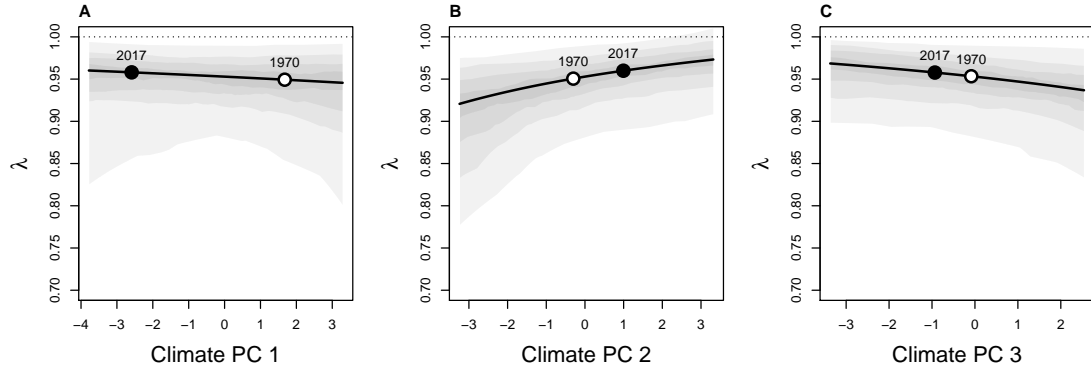


Figure 3: Predicted asymptotic population growth rate (λ) in response to three principal components of inter-annual climatic variation (A-C). For each panel, the indicated principal component is varying while the others are held at zero (the average value). Lines show the expected relationships based on posterior mean parameter values and shaded contours show the 25,50,75, and 95% credible intervals, representing uncertainty in demographic parameters. Points highlight the change the PC value (on the x -axis) between 1970 and 2017, based on the regression lines shown in Fig. 1, and the predicted corresponding change in λ (y -axis).

Back-casting population growth

Figure 4A shows the back-casted time series of λ accounting for inter-annual variation in all three PC components. For the observation years (2004-2017), the three climate PCs explained 60% of the inter-annual variation in λ (points in Fig. 4A). Thus, even with relatively strong climate-demography associations (Fig. 2), there was substantial uncertainty in our back-casted estimates of λ . The shaded region in Fig. 4A represents the combined uncertainty arising from heterogeneity in vital rates across years that could not be attributed to the climate PCs (process error) and imperfect knowledge of the underlying parameters (estimation error). In Appendix Fig. C3, we show that process error contributed the majority of the

350 total uncertainty.

351 Despite uncertainty in our back-cast, the results indicated that λ has likely
352 remained below replacement levels for more than a century; there was no evidence
353 that climate change drove this population into extinction debt. To the contrary,
354 there was a positive temporal trend ($\frac{\Delta\lambda}{\Delta Year} > 0$), suggesting a trajectory of increas-
355 ing population growth rates through time (Fig. 4B). There was wide uncertainty
356 in the rate of change but the posterior probability distribution indicated that it
357 was 2.5 times more likely that λ has increased than decreased. Furthermore, the
358 median rate of increase was 2.27 times greater since 1970 compared to the overall
359 trend since 1900 (Fig. 4B), corresponding to the acceleration of climate change
360 (Fig. 1). There was greater uncertainty in $\frac{\Delta\lambda}{\Delta Year}$ since 1970 because this estimate
361 was based on fewer years. Under the trajectory since 1970, population growth
362 was expected to reach the viability threshold ($\lambda = 1$) in the year 2057 (Fig. 4C);
363 accelerating climate change would advance this transition to viable growth rates.

364 In Appendix D, we show that our inference that λ is likely increasing in response
365 to climate change holds even with a more conservative approach that does not
366 extrapolate vital rate responses beyond the climate extremes of the observation
367 years. Furthermore, in Appendix A, we show that year-specific estimates of λ
368 were correlated between models built with downscaled climate data versus on-site
369 meteorological measurements, for years in which they over-lapped (Fig. A7). This
370 suggests that our qualitative inference regarding the positive temporal trend in λ
371 is robust to the loss of resolution associated with downscaled climate data.

372 The stochastic population growth rate (λ_S) showed a similar trend of $\lambda_S < 1$
373 and increasing population growth rates over the past 120 years (Fig. C4). The
374 stochastic growth rate reveals the effects of multi-year climate events, such as the

375 runs of good years in the 1940s and 2000s.

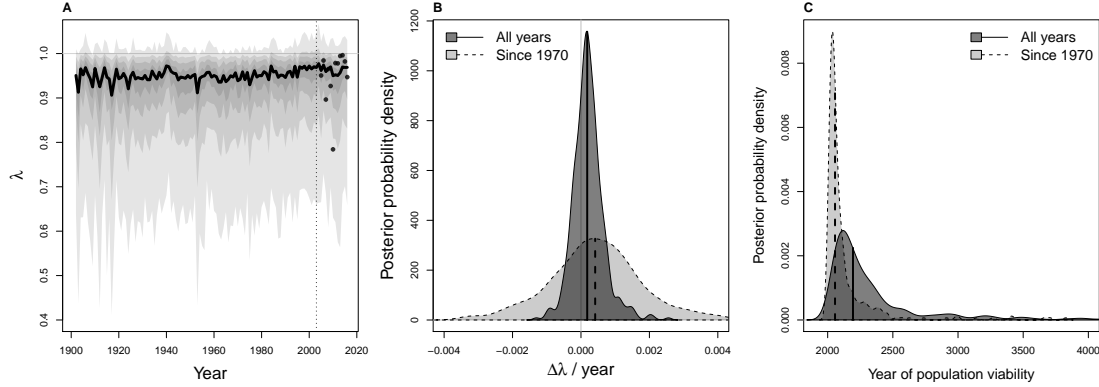


Figure 4: **A**, Posterior probability distribution for the time series of asymptotic population growth rates (λ) predicted based on inter-annual variation in three climate PCs. Thick black line shows the mean prediction and shaded regions show the 25, 50, 75, and 95% credible regions accounting for both parameter uncertainty and process error (year-to-year variation in vital rates that was unrelated to climate). Dashed vertical line separates years that were back-casted versus years that were directly observed. The observation years (2004 and later) include estimates for year-specific population growth rates (points), captured statistically as year-specific random effects in the vital rates. **B**, Posterior distributions for the rate of temporal change in population growth ($\frac{\Delta\lambda}{\Delta Y_{\text{year}}}$). Dark grey shows the rate of change across all years shown in **A** and light grey shows the rate of change since 1970. Vertical lines show median values. **C**, Posterior distributions for the year of population viability ($\lambda = 1$) for the subset of posterior samples for which $\frac{\Delta\lambda}{\Delta Y_{\text{year}}} > 0$. Shading and lines as in **B**.

376 Life Table Response Experiment

377 Life Table Response Experiments (LTRE) provided a decomposition of how λ
 378 responded to long-term climate trends (1900-2017), allowing us to understand the
 379 relative importance of different dimensions of climate variability and vital rate
 380 responses to them. LTRE results indicated that survival responses to climate
 381 were the overwhelming driver of temporal trends in λ (Fig. 5). Individual growth

made no contribution to these trends because it was unresponsive to climate (Fig. D,E,F), whereas flowering and fertility were responsive to climate but their role was relatively small and imperceptible in Fig. 5. Furthermore, survival responses to climate PC2 were the dominant driver of temporal trends, followed by PC3 and then PC1. Collectively, responses to PC2 and PC3 accounted for 91% of the overall climate effect in back-casted values of λ .

Discussion

Understanding and predicting the effects of environmental change on plant demography and population dynamics are urgent challenges. The integration of long-term data with environmentally explicit demographic models provides a powerful vehicle for meeting these challenges and may aid in identifying processes that drive some populations into decline. By reconstructing 117 years of climate-dependent demography, we tested the hypothesis that the extinction debt of our study population was a consequence of recent climate change. Our results suggest the opposite: *C. imbricata* is likely a climate change “winner”, on an accelerating trajectory toward replacement-level population growth within 37 years if current climate change trends persist, and sooner if they accelerate. We further show that the strongest feature of climate change in this system was not the main driver of population responses. Instead, temporal trends in population viability were dominated by more subtle climatic factors with relatively weak signals of recent change. Below, we interpret these results in greater detail and discuss their broader significance.

Until recently, few plant demographic studies explicitly considered climatic drivers of inter-annual variation (Ehrlén *et al.*, 2016; Crone *et al.*, 2011), though

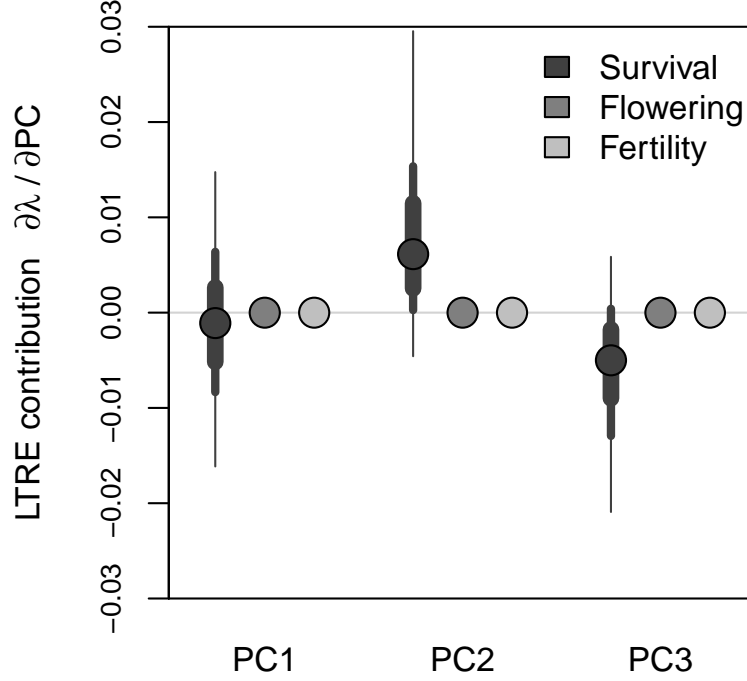


Figure 5: LTR decomposition of climate-driven inter-annual variability in population growth rates. Lines of decreasing thickness show the 50, 75 and 95 percentiles of the posterior distributions of the vital rate parameters, and points show the median. Shading corresponds to different vital rates (survival, flowering, and fertility) Posterior distributions for flowering and fertility are imperceptible on this scale.

405 this is rapidly changing. We are aware of no previous studies that have compared
 406 the magnitudes of different aspects of climate change alongside the magnitudes of
 407 demographic responses to those changes. However, we suspect that our key finding
 408 – that the strongest dimension of climate change was not the strongest driver of

409 demography – may be common, since at the heart of this result lies the difference
410 between annual climate trends (captured by PC1) versus seasonal trends (PCs 2
411 and 3). Annual rainfall totals in our region have been decreasing but more of the
412 annual rainfall has been falling in the cool season, consistent with previous climata-
413 logical studies that suggest a shift from warm- to cool-season precipitation (Cook &
414 Seager, 2013; Cook *et al.*, 2015; Petrie *et al.*, 2014). Similarly, annual temperatures
415 have been increasing in our study region but it was cool-season warming, specif-
416 ically, that was most important for *C. imbricata* demography. Many plant and
417 animal life histories operate on seasonal schedules and may therefore be more sen-
418 sitive to seasonal redistribution of rainfall and temperature than to climate effects
419 that manifest over an entire year. Our results are consistent with previous studies
420 that demonstrate the importance of considering seasonal, not annual, drivers of
421 plant demographic responses (Selwood *et al.*, 2015; Williams *et al.*, 2015; Dahlgren
422 *et al.*, 2016). Some recent studies have taken a finer-grained approach, connecting
423 plant responses to weather events on monthly, weekly, or even daily time scales
424 (Teller *et al.*, 2016; Tenhumberg *et al.*, 2018; Shriver, 2016). For tractability, we
425 did not explore lagged climate effects beyond one year, though methods for doing
426 so are rapidly developing (Teller *et al.*, 2016; Tenhumberg *et al.*, 2018; Ogle *et al.*,
427 2015). Finding the appropriate timing and resolution of climate covariates is an
428 important area for future work in this system and more generally.

429 Rigorously accounting for various types of uncertainty is another an important
430 area in the development of environmentally explicit models for forecasting or back-
431 casting. Even with strong climate-demography relationships detected with our
432 unusually long-term data set, climate drivers accounted for **less than two-thirds** of
433 the inter-annual variation in λ during the study years. It was therefore important

434 to place our predictions for historical growth rates in the context of the substantial
435 uncertainty that arose from process error: all the additional, unspecified ways
436 that years may differ. We have emphasized the positive trajectory of population
437 viability as the most likely trend in λ , but this should be interpreted in light
438 of the probability distributions that we provide (Fig. 4) – that is, with nuance
439 and appropriate caution¹. As ecologists are increasingly called upon to forecast
440 responses to change in climate drivers, it will be essential to do so in a probabilistic
441 framework that accommodates process error, i.e., the variability *not* explained by
442 climate drivers. Defining the temporal or spatial auto-correlation structure of
443 process error (which we did not attempt) may further improve forecasts or back-
444 casts.

445 Different aspects of a species' life cycle may respond in diverse ways to environ-
446 mental drivers (Doak & Morris, 2010; Villellas *et al.*, 2015), highlighting the addi-
447 tional importance of considering multiple vital rates for understanding responses
448 to global change. Our work was able to pinpoint which responses throughout the
449 life cycle were most important for the overall population response to climate. Our
450 results are consistent with previous findings that high-sensitivity vital rates (those
451 that strongly influence λ , in this case survival and growth) are buffered against en-
452 vironmental variability while low-sensitivity vital rates (flowering and fertility) may
453 exhibit wide fluctuations (Pfister, 1998). However, incomplete buffering of survival
454 led to greater mortality in years with cold and dry cool-seasons – years that are be-
455 coming less frequent under climate change (Fig. 1) – and these survival responses
456 dominated the overall increase in population viability over the past 120 years

¹By coincidence, the probability that λ is increasing (0.714) matched the probability of a Clinton victory in the 2016 U.S. presidential election: <https://projects.fivethirtyeight.com/2016-election-forecast/>

(Fig. 5). These results mirror a recent study of another long-lived perennial plant, the alpine sunflower *Helianthella quinquinervis*, where reproductive responses to climate drivers were strong but ultimately overwhelmed by weaker responses in survival that more strongly affected population growth (Iler *et al.*, 2019). It is commonly observed that demographic transitions related to growth and survival are the most important determinants of population viability in species with long-lived perennial life histories (Franco & Silvertown, 2004). It may therefore be a general result that climate effects on growth and survival will be more consequential in long-lived perennials than effects on reproductive processes, even as the latter exhibit greater sensitivity to climate, since perennials have many reproductive opportunities over potentially long lifespans (Dalglish *et al.*, 2010; Morris *et al.*, 2008).

Our historical reconstruction of climate-dependent population growth indicated that the climate has likely never been better for *C. imbricata* than it is now. This result begs the question of how these plants have reached their current, relatively high abundance, given over a century of population growth rates that were inferred to fall well below replacement levels. Land use history – which is not incorporated into our back-casted estimates – may have played a role. The Sevilleta NWR was exposed to grazing for much of the 20th century until 1973. Previous work suggests that cacti, and *C. imbricata* in particular, can increase in abundance in response to grazing, due to livestock dispersing detached stem segment and thus promoting asexual regeneration (Allen *et al.*, 1991). During our study, we observed recruitment to be almost exclusively from seed (sexual and asexual recruits are easily distinguishable), though it is possible that regeneration dynamics were different under historical grazing regimes. Grazing may have also promoted

cactus populations through release of competitive interactions with grasses (Yu
 $et al.$, 2019). Thus, one hypothesis is that *C. imbricata* achieved current densities
under the historical land use regime, and cannot maintain these densities in the
absence of cattle grazing. For long-lived plants, it may take decades to centuries
for full payment of extinction debt driven by land use changes (Lehtilä $et al.$,
2016; González-Varo $et al.$, 2015). An alternative hypothesis is that, independent
of grazing or other land use history, our study population may be located in sink
habitat and maintained by dispersal from nearby populations that are more viable.
Indeed, previous work showed that *C. imbricata* at lower (by ca. 100 m) elevations
had positive population growth rates (Miller $et al.$, 2009) and may therefore act
as source populations. Regardless of which process or processes best account for
the persistence of a population that is currently inviable, our results indicate that
it will more likely than not be ‘rescued’ by ongoing climate change. One caveat
to this conclusion is that, beyond the mean climate trends we have described, fu-
ture climate (and especially monsoon precipitation) in our region is expected to
be more variable (Rudgers $et al.$, 2018; Cook $et al.$, 2015) and this may dampen
population growth independently of mean conditions (Boyce $et al.$, 2006). How-
ever, our stochastic demographic analysis, which accounts for increasing climate
variability during the 20th century, also showed a positive trajectory of λ_S (Fig.
C4).

Previous studies of cacti have emphasized their sensitivity to freezing as a con-
straint on physiological performance and geographic distribution (Flores & Yeaton,
2003; Kinraide, 1978; Nobel, 1984). In our study, we detected an important role
for winter minimum temperature and observed high mortality following record low
winter temperatures over a multi-day deep-freeze in 2011 (this is the low outlier

507 in Fig. 4A). As these freezing events become less frequent under climate change,
508 we expect an increase in regional abundance and perhaps northern expansion of
509 *C. imbricata*'s range, which currently extends to southern Colorado and is likely
510 limited by winter minimum temperatures. This may be an issue of applied concern
511 in the region since *C. imbricata* is considered undesirable **due to its unpalatabil-**
512 **ity to livestock** (Allen *et al.*, 1991). The role of cool-season precipitation that we
513 detected was more surprising. A majority of annual precipitation in the South-
514 west US comes from warm-season monsoon events (Adams & Comrie, 1997) and
515 these events play a critical role in vegetation dynamics (Notaro & Gutzler, 2012;
516 Petrie *et al.*, 2014), especially for plants with C4 and CAM photosynthesis that
517 are physiologically most active during the warm summer months. Previous cactus
518 demographic studies have emphasized the role of summer monsoon precipitation
519 (Winkler *et al.*, 2018; Bowers, 2005). Our results suggest that, despite its summer-
520 adapted CAM photosynthetic pathway, *C. imbricata* is able to capitalize on cool-
521 season moisture, and this was an important component of the positive demographic
522 effects of recent climate change. Similarly, Salguero-Gomez *et al.* (2012) identified
523 *Cryptantha flava* as **a species likely to benefit from climate change** due in part to
524 seasonal redistribution of rainfall that will lengthen its growing season.

525 Our work highlights several considerations that may be relevant for studies of
526 demographic back-casting in other systems. First, we faced a trade-off between
527 temporal depth and local resolution of climate data. While downscaled climate
528 interpolation (from ClimateWNA) and on-site measurements (from SEV-LTER)
529 were correlated, they were not perfectly so (Appendix A); this was especially true
530 for temperature minima and maxima (Table A1), where downscaled data likely
531 mis-estimate localized extremes. We prioritized the greater temporal coverage

provided by downscaled data, which led an 18% reduction in how well climate explained inter-annual variation in λ , relative to on-site climate data (Appendix A). Consequently, reliance on downscaled data inflated the contribution of process error to our back-casted estimates (Appendix D), and made λ appear less responsive to climate than it likely was. It is particularly noteworthy that the downscaled climate data poorly captured the deep-freeze of winter 2011 (Fig. A1A). Poor demographic performance in this year was consequently attributed to a statistical random effect (Fig. 4A), though this was almost certainly a true climate effect. As expected, the on-site data predicted a lower λ value in this year than the downscaled data (Fig. A7). When available, climate data sources that break the trade-off between temporal depth and local resolution would provide the strongest foundation for accurate back-casting. When such resources are not available, quantifying the loss of resolution, as we have done (Appendix A), may be valuable for interpreting results.

Second, just like forecasting, demographic back-casting may require projection into climatic conditions that were represented poorly or not at all during the data collection period. This requires the assumption that the relationship between vital rates and climate covariates does not change or break down under conditions more extreme than observed. We found similar results whether or not we extrapolated demographic performance into unobserved conditions (Appendix D). This was a lucky break, reflecting the fact that the climate covariate requiring the most extrapolation (PC1) had the weakest effect on λ . In other cases, where important covariates must be extrapolated to no-analogue conditions, comparing results with and without extrapolation (Appendix D) may be valuable for setting liberal and conservative bounds on model projections. This approach may also aid in identi-

557 fying situations where experimental climate manipulations could help bridge the
558 gap between current and historic (or future) conditions.

559 Some additional limitations of our study warrant consideration in the inter-
560 pretation of our results. First, our treatment of climate dependence was limited
561 to four vital rate processes of established plants. Because we could not reliably
562 assign a birth year to new recruits, we did not incorporate climate dependence in
563 seedling recruitment. Previous studies of cactus demography suggest that seedling
564 recruitment may be highly sensitive to climate, especially monsoon precipitation
565 (e.g., Bowers 2005; Winkler *et al.* 2018). We suspect this is the case for *C. imbrica-*
566 *tata*, since germination usually coincides with late-summer rains (*T.E.X. Miller,*
567 *unpubl. data*). Because we did not model this process as climate-dependent, our
568 results for climate effects on population growth are conservative. However, con-
569 sistent with expectations for long-lived perennials, we know seedling recruitment
570 to have very low eigenvalue sensitivities (Elder & Miller, 2016), which suggests
571 that even large climate effects on this process may not strongly register in terms of
572 population growth. On the other hand, pulsed recruitment events perturb the size
573 distribution in ways that can importantly affect short-term (transient) dynamics
574 (Williams *et al.*, 2011), and may therefore warrant further study in this and other
575 pulsed-recruitment system.

576 To conclude, this study illustrates how long-term patterns of population growth
577 can be reconstructed through climate-demography relationships observed on rel-
578 atively short time scales. This allowed us to evaluate the hypothesis that recent
579 climate change has driven *C. imbricata* in our region into extinction debt, a hypoth-
580 esis that our data do not support. Instead, this species is most likely benefitting
581 from climate change, largely due to its positive responses, especially in survival, to

582 recent and ongoing shifts in cool-season temperature and precipitation. Changes
583 in cool-season climate were not the strongest features of climate change, but they
584 were nonetheless the most important determinants of population responses. The
585 more general lesson for global change biologists is that relatively subtle dimensions
586 of climate change may trigger strong ecological responses.

587 **Acknowledgements**

588 This study was supported by the Sevilleta LTER (NSF LTER awards 1440478,
589 1655499, and 1748133) and by NSF Division of Environmental Biology awards
590 1543651 and 1754468. We thank the Sevilleta National Wildlife Refuge staff (es-
591 pecially J. Erz) for facilitating research access. We thank M. Evans and E. Schultz
592 for helpful discussions on modeling climate-demography relationships. Finally, we
593 thank the many students and colleagues have contributed to this long-term study,
594 especially M. Donald, A. Compagnoni, and B. Ochocki. Two reviewers provided
595 helpful feedback on our work.

596 **Author contributions**

597 TEXM initiated and maintains the long-term study. KC collected and analyzed
598 data and prepared a manuscript draft. TEXM finalized text and analyses. Both
599 coauthors approve this submission.

Data accessibility

All of the code for our statistical and demographic modeling is available at https://github.com/texmiller/cholla_climate_IPM and raw data will be published in parallel with this manuscript.

References

- Ådahl E, Lundberg P, Jonzen N (2006) From climate change to population change: the need to consider annual life cycles. *Global Change Biology*, **12**, 1627–1633.
- Adams DK, Comrie AC (1997) The north american monsoon. *Bulletin of the American Meteorological Society*, **78**, 2197–2214.
- Adler PB, Byrne KM, Leiker J (2013) Can the past predict the future? experimental tests of historically based population models. *Global change biology*, **19**, 1793–1803.
- Allen L, Allen E, Kunst C, Sosebee R (1991) A diffusion model for dispersal of *Opuntia imbricata* (cholla) on rangeland. *The Journal of Ecology*, pp. 1123–1135.
- Bowers JE (2005) Influence of climatic variability on local population dynamics of a sonoran desert *Platyopuntia*. *Journal of Arid Environments*, **61**, 193–210.
- Boyce MS, Haridas CV, Lee CT, Group NSDW, *et al.* (2006) Demography in an increasingly variable world. *Trends in Ecology & Evolution*, **21**, 141–148.
- Buckley LB, Kingsolver JG (2012) The demographic impacts of shifts in climate means and extremes on alpine butterflies. *Functional Ecology*, **26**, 969–977.

- 620 Caswell H (2001) *Matrix Population Models*. Sinauer Associates, Inc., Sunderland,
621 MA, 2 edn.
- 622 Compagnoni A, Bibian AJ, Ochocki BM, *et al.* (2016) The effect of demographic
623 correlations on the stochastic population dynamics of perennial plants. *Ecolog-
624 ical Monographs*, **86**, 480–494.
- 625 Cook B, Seager R (2013) The response of the north american monsoon to increased
626 greenhouse gas forcing. *Journal of Geophysical Research: Atmospheres*, **118**,
627 1690–1699.
- 628 Cook BI, Ault TR, Smerdon JE (2015) Unprecedented 21st century drought risk
629 in the american southwest and central plains. *Science Advances*, **1**, e1400082.
- 630 Crone EE, Menges ES, Ellis MM, *et al.* (2011) How do plant ecologists use matrix
631 population models? *Ecology letters*, **14**, 1–8.
- 632 Dahlgren JP, Bengtsson K, Ehrlén J (2016) The demography of climate-driven and
633 density-regulated population dynamics in a perennial plant. *Ecology*.
- 634 Dalglish HJ, Koons DN, Adler PB (2010) Can life-history traits predict the re-
635 sponse of forb populations to changes in climate variability? *Journal of Ecology*,
636 **98**, 209–217.
- 637 Dalglish HJ, Koons DN, Hooten MB, Moffet CA, Adler PB (2011) Climate influ-
638 ences the demography of three dominant sagebrush steppe plants. *Ecology*, **92**,
639 75–85.
- 640 Daly C, Halbleib M, Smith JI, *et al.* (2008) Physiographically sensitive mapping
641 of climatological temperature and precipitation across the conterminous united

- 642 states. *International Journal of Climatology: a Journal of the Royal Meteorological Society*, **28**, 2031–2064.
- 643
- 644 Dinno A (2018) *paran: Horn's Test of Principal Components/Factors*. URL <https://CRAN.R-project.org/package=paran>. R package version 1.5.2.
- 645
- 646 Doak DF, Morris WF (2010) Demographic compensation and tipping points in
- 647 climate-induced range shifts. *Nature*, **467**, 959.
- 648 Dullinger S, Gatttringer A, Thuiller W, *et al.* (2012) Extinction debt of high-
- 649 mountain plants under twenty-first-century climate change. *Nature Climate*
- 650 *Change*, **2**, 619.
- 651 Dybala KE, Eadie JM, Gardali T, Seavy NE, Herzog MP (2013) Projecting de-
- 652 mographic responses to climate change: adult and juvenile survival respond
- 653 differently to direct and indirect effects of weather in a passerine population.
- 654 *Global Change Biology*, **19**, 2688–2697.
- 655 Ehrlén J, Morris WF (2015) Predicting changes in the distribution and abundance
- 656 of species under environmental change. *Ecology Letters*, **18**, 303–314.
- 657 Ehrlén J, Morris WF, von Euler T, Dahlgren JP (2016) Advancing environmentally
- 658 explicit structured population models of plants. *Journal of Ecology*, **104**, 292–
- 659 305.
- 660 Elderd BD, Miller TE (2016) Quantifying demographic uncertainty: Bayesian
- 661 methods for integral projection models. *Ecological Monographs*, **86**, 125–144.
- 662 Flores JL, Yeaton R (2003) The replacement of arborescent cactus species along a

663 climatic gradient in the southern chihuahuan desert: competitive hierarchies and
664 response to freezing temperatures. *Journal of arid environments*, **55**, 583–594.

665 Franco M, Silvertown J (2004) A comparative demography of plants based upon
666 elasticities of vital rates. *Ecology*, **85**, 531–538.

667 Franklin SB, Gibson DJ, Robertson PA, Pohlmann JT, Fralish JS (1995) Parallel
668 analysis: a method for determining significant principal components. *Journal of*
669 *Vegetation Science*, **6**, 99–106.

670 Frederiksen M, Daunt F, Harris MP, Wanless S (2008) The demographic impact
671 of extreme events: stochastic weather drives survival and population dynamics
672 in a long-lived seabird. *Journal of Animal Ecology*, **77**, 1020–1029.

673 George EI, McCulloch RE (1993) Variable selection via gibbs sampling. *Journal*
674 *of the American Statistical Association*, **88**, 881–889.

675 González-Varo JP, Albaladejo RG, Aizen MA, Arroyo J, Aparicio A (2015) Ex-
676 tinction debt of a common shrub in a fragmented landscape. *Journal of Applied*
677 *Ecology*, **52**, 580–589.

678 Hastings A, Abbott KC, Cuddington K, *et al.* (2018) Transient phenomena in
679 ecology. *Science*, **361**, eaat6412.

680 Hijmans RJ, Cameron SE, Parra JL, Jones PG, Jarvis A (2005) Very high reso-
681 lution interpolated climate surfaces for global land areas. *International Journal*
682 *of Climatology: A Journal of the Royal Meteorological Society*, **25**, 1965–1978.

683 Hooten MB, Hobbs N (2015) A guide to bayesian model selection for ecologists.
684 *Ecological Monographs*, **85**, 3–28.

- Hylander K, Ehrlén J (2013) The mechanisms causing extinction debts. *Trends in ecology & evolution*, **28**, 341–346.
- Iler AM, Compagnoni A, Inouye DW, Williams JL, CaraDonna PJ, Anderson A, Miller TE (2019) Reproductive losses due to climate change-induced earlier flowering are not the primary threat to plant population viability in a perennial herb. *Journal of Ecology*, **107**, 1931–1943.
- Jenouvrier S, Caswell H, Barbraud C, Holland M, Stroeve J, Weimerskirch H (2009) Demographic models and ipcc climate projections predict the decline of an emperor penguin population. *Proceedings of the National Academy of Sciences*, **106**, 1844–1847.
- Jenouvrier S, Holland M, Stroeve J, Serreze M, Barbraud C, Weimerskirch H, Caswell H (2014) Projected continent-wide declines of the emperor penguin under climate change. *Nature Climate Change*, **4**, 715.
- Kinraide TB (1978) The ecological distribution of cholla cactus (*opuntia imbricata* (haw.) dc.) in el paso county, colorado. *The Southwestern Naturalist*, pp. 117–133.
- Kuussaari M, Bommarco R, Heikkinen RK, *et al.* (2009) Extinction debt: a challenge for biodiversity conservation. *Trends in ecology & evolution*, **24**, 564–571.
- Lehtilä K, Dahlgren JP, Garcia MB, Leimu R, Syrjänen K, Ehrlén J (2016) Forest succession and population viability of grassland plants: long repayment of extinction debt in *primula veris*. *Oecologia*, **181**, 125–135.
- Lynch HJ, Rhainds M, Calabrese JM, Cantrell S, Cosner C, Fagan WF (2014) How

707 climate extremes—not means—define a species’ geographic range boundary via
 708 a demographic tipping point. *Ecological Monographs*, **84**, 131–149.

709 Maschinski J, Baggs JE, QUINTANA-ASCENCIO PF, Menges ES (2006) Using
 710 population viability analysis to predict the effects of climate change on the ex-
 711 tinction risk of an endangered limestone endemic shrub, arizona cliffrose. *Con-
 712 servation Biology*, **20**, 218–228.

713 McLean N, Lawson CR, Leech DI, van de Pol M (2016) Predicting when climate-
 714 driven phenotypic change affects population dynamics. *Ecology Letters*, **19**,
 715 595–608.

716 Miller TE, Louda SM, Rose KA, Eckberg JO (2009) Impacts of insect herbivory on
 717 cactus population dynamics: experimental demography across an environmental
 718 gradient. *Ecological Monographs*, **79**, 155–172.

719 Morris WF, Pfister CA, Tuljapurkar S, *et al.* (2008) Longevity can buffer plant and
 720 animal populations against changing climatic variability. *Ecology*, **89**, 19–25.

721 Morrison SF, Hik DS (2007) Demographic analysis of a declining pika ochotona
 722 collaris population: linking survival to broad-scale climate patterns via spring
 723 snowmelt patterns. *Journal of Animal ecology*, **76**, 899–907.

724 Nobel PS (1984) Extreme temperatures and thermal tolerances for seedlings of
 725 desert succulents. *Oecologia*, **62**, 310–317.

726 Notaro M, Gutzler D (2012) Simulated impact of vegetation on climate across the
 727 north american monsoon region in ccs3. 5. *Climate dynamics*, **38**, 795–814.

- 728 Ogle K, Barber JJ, Barron-Gafford GA, *et al.* (2015) Quantifying ecological mem-
729 ory in plant and ecosystem processes. *Ecology letters*, **18**, 221–235.
- 730 Ohm JR, Miller TE (2014) Balancing anti-herbivore benefits and anti-pollinator
731 costs of defensive mutualists. *Ecology*, **95**, 2924–2935.
- 732 Peters DP, Havstad KM, Archer SR, Sala OE (2015) Beyond desertification: new
733 paradigms for dryland landscapes. *Frontiers in Ecology and the Environment*,
734 **13**, 4–12.
- 735 Petrie M, Collins S, Gutzler D, Moore D (2014) Regional trends and local variabil-
736 ity in monsoon precipitation in the northern chihuahuan desert, usa. *Journal of*
737 *arid environments*, **103**, 63–70.
- 738 Pfister CA (1998) Patterns of variance in stage-structured populations: evolution-
739 ary predictions and ecological implications. *Proceedings of the National Academy*
740 *of Sciences*, **95**, 213–218.
- 741 Plummer M, *et al.* (2003) Jags: A program for analysis of bayesian graphical
742 models using gibbs sampling. In: *Proceedings of the 3rd international workshop*
743 *on distributed statistical computing*, vol. 124. Vienna, Austria.
- 744 Rudgers JA, Chung YA, Maurer GE, Moore DI, Muldavin EH, Litvak ME, Collins
745 SL (2018) Climate sensitivity functions and net primary production: A frame-
746 work for incorporating climate mean and variability. *Ecology*, **99**, 576–582.
- 747 Salguero-Gomez R, Siewert W, Casper BB, Tielbörger K (2012) A demographic
748 approach to study effects of climate change in desert plants. *Philosophical Trans-*
749 *actions of the Royal Society B: Biological Sciences*, **367**, 3100–3114.

- 750 Selwood KE, McGeoch MA, Mac Nally R (2015) The effects of climate change
751 and land-use change on demographic rates and population viability. *Biological*
752 *Reviews*, **90**, 837–853.
- 753 Shriver RK (2016) Quantifying how short-term environmental variation leads to
754 long-term demographic responses to climate change. *Journal of Ecology*, **104**,
755 65–78.
- 756 Sletvold N, Dahlgren JP, Øien DI, Moen A, Ehrlén J (2013) Climate warming alters
757 effects of management on population viability of threatened species: results from
758 a 30-year experimental study on a rare orchid. *Global Change Biology*, **19**, 2729–
759 2738.
- 760 Smith M, Caswell H, Mettler-Cherry P (2005) Stochastic flood and precipitation
761 regimes and the population dynamics of a threatened floodplain plant. *Ecological*
762 *Applications*, **15**, 1036–1052.
- 763 Su YS, Yajima M (2012) R2jags: A package for running jags from r. *R package*
764 *version 0.03-08*, URL <http://CRAN.R-project.org/package=R2jags>.
- 765 Teller BJ, Adler PB, Edwards CB, Hooker G, Ellner SP (2016) Linking demogra-
766 phy with drivers: climate and competition. *Methods in Ecology and Evolution*,
767 **7**, 171–183.
- 768 Tenhumberg B, Crone EE, Ramula S, Tyre AJ (2018) Time-lagged effects of
769 weather on plant demography: drought and astragalus scaphoides. *Ecology*,
770 **99**, 915–925.

- Urban MC (2015) Accelerating extinction risk from climate change. *Science*, **348**, 571–573.
- Van de Pol M, Vindenes Y, Sæther BE, Engen S, Ens BJ, Oosterbeek K, Tinbergen JM (2010) Effects of climate change and variability on population dynamics in a long-lived shorebird. *Ecology*, **91**, 1192–1204.
- Vellend M, Verheyen K, Jacquemyn H, Kolb A, Van Calster H, Peterken G, Hermy M (2006) Extinction debt of forest plants persists for more than a century following habitat fragmentation. *Ecology*, **87**, 542–548.
- Villellas J, Doak DF, García MB, Morris WF (2015) Demographic compensation among populations: what is it, how does it arise and what are its implications? *Ecology letters*, **18**, 1139–1152.
- Wang T, Hamann A, Spittlehouse D, Carroll C (2016) Locally downscaled and spatially customizable climate data for historical and future periods for north america. *PLoS One*, **11**, e0156720.
- Williams JL, Ellis MM, Bricker MC, Brodie JF, Parsons EW (2011) Distance to stable stage distribution in plant populations and implications for near-term population projections. *Journal of ecology*, **99**, 1171–1178.
- Williams JL, Jacquemyn H, Ochocki BM, Brys R, Miller TE (2015) Life history evolution under climate change and its influence on the population dynamics of a long-lived plant. *Journal of Ecology*, **103**, 798–808.
- Williams JL, Miller TEX, Ellner SP (2012) Avoiding unintentional eviction from integral projection models. *Ecology*, **93**, 2008–2014.

- 793 Winkler DE, Conner JL, Huxman TE, Swann DE (2018) The interaction of drought
794 and habitat explain space–time patterns of establishment in saguaro (*Carnegiea*
795 *gigantea*). *Ecology*, **99**, 621–631.
- 796 Yu K, D’Odorico P, Collins SL, *et al.* (2019) The competitive advantage of a con-
797 stitutive cam species over a C4 grass species under drought and CO2 enrichment.
798 *Ecosphere*, **10**, e02721.

Appendix A: Correspondence between downscaled and locally measured climate variables

Correlation of climate values

We compared warm- and cool-season values of four climate variables (total precipitation and minimum, mean, and maximum temperature) between two data sources: the SEV-LTER meteorological station nearest our study site (station 50 in the SEV-LTER meteorological network) and downscaled data from ClimateWNA corresponding to the same latitude, longitude, and elevation as station 50. Our goal was to determine how well the downscaled data captured conditions ‘on the ground’ as measured directly by the meteorological station. We compared the years 2001 through 2017, which are the years of overlap between the two data sources.

There was moderate to strong agreement between the two data sources (Table A1, Fig. A1, Fig. A2). Temperature extrema were less strongly correlated between the two data sets than temperature means (Fig. A1), which is unsurprising given that extreme values may be sensitive to local micro-environmental conditions that the relatively coarse downscaled data would miss. There was an extreme-cold event in 2011 that was particularly poorly captured by the downscaled data (Fig. A1A). The weakest correlation was that of warm-season maximum temperature (Fig. A1F; Pearson’s $r = 0.41$, $P = 0.11$).

Table A1: Correlations between seasonal climate values measured by an on-site meteorological station versus downscaled data from ClimateWNA corresponding to the same years and location. Correlation values show Pearson correlations and P-values come from t -tests with 14 degrees of freedom.

Season	Variable	Correlation	P-value
Warm	Min temperature	0.59	0.0153
Warm	Mean temperature	0.84	10^{-4}
Warm	Max temperature	0.41	0.1135
Warm	Precipitation	0.49	0.0544
Cool	Min temperature	0.51	0.0622
Cool	Mean temperature	0.94	3.6×10^{-7}
Cool	Max temperature	0.69	0.0069
Cool	Precipitation	0.87	4.6×10^{-5}

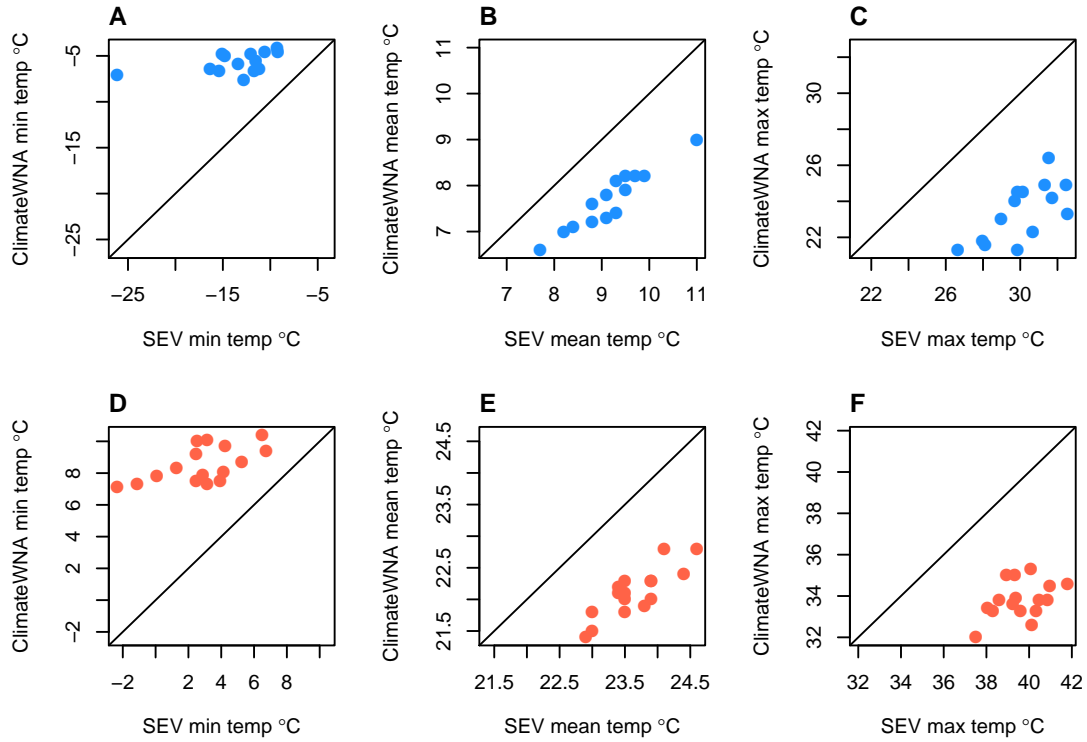


Figure A1: Correlations of minimum, mean, and maximum temperature values of cool (A–C) and warm (D–F) seasons between SEV-LTER meteorological data and downscaled estimates from ClimateWNA for years 2004–2017. Diagonal lines show $y = x$.

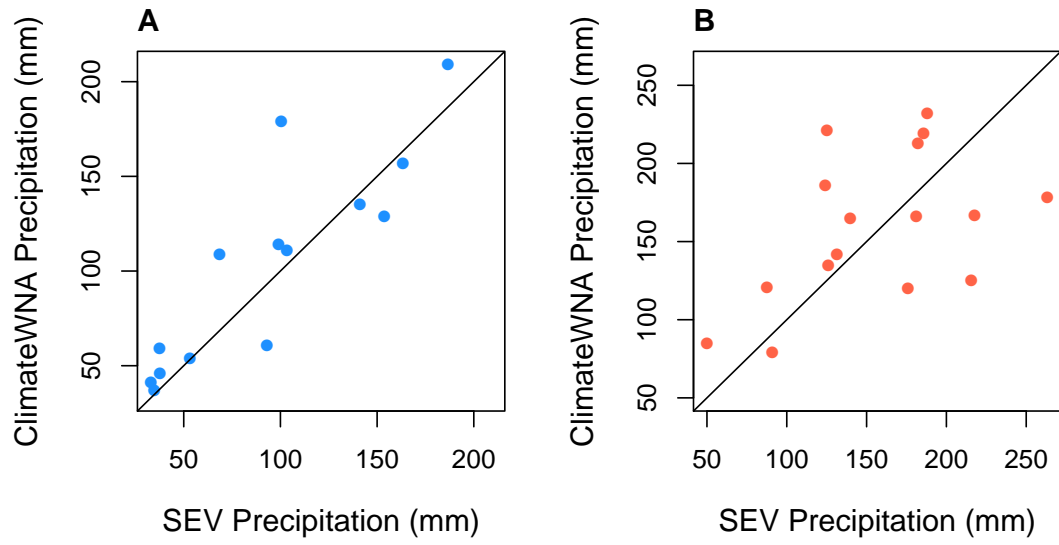


Figure A2: Correlations of cool- (**A**) and warm-season (**B**) precipitation between SEV-LTER meteorological data and downscaled estimates from ClimateWNA for years 2004–2017. Diagonal lines show $y = x$.

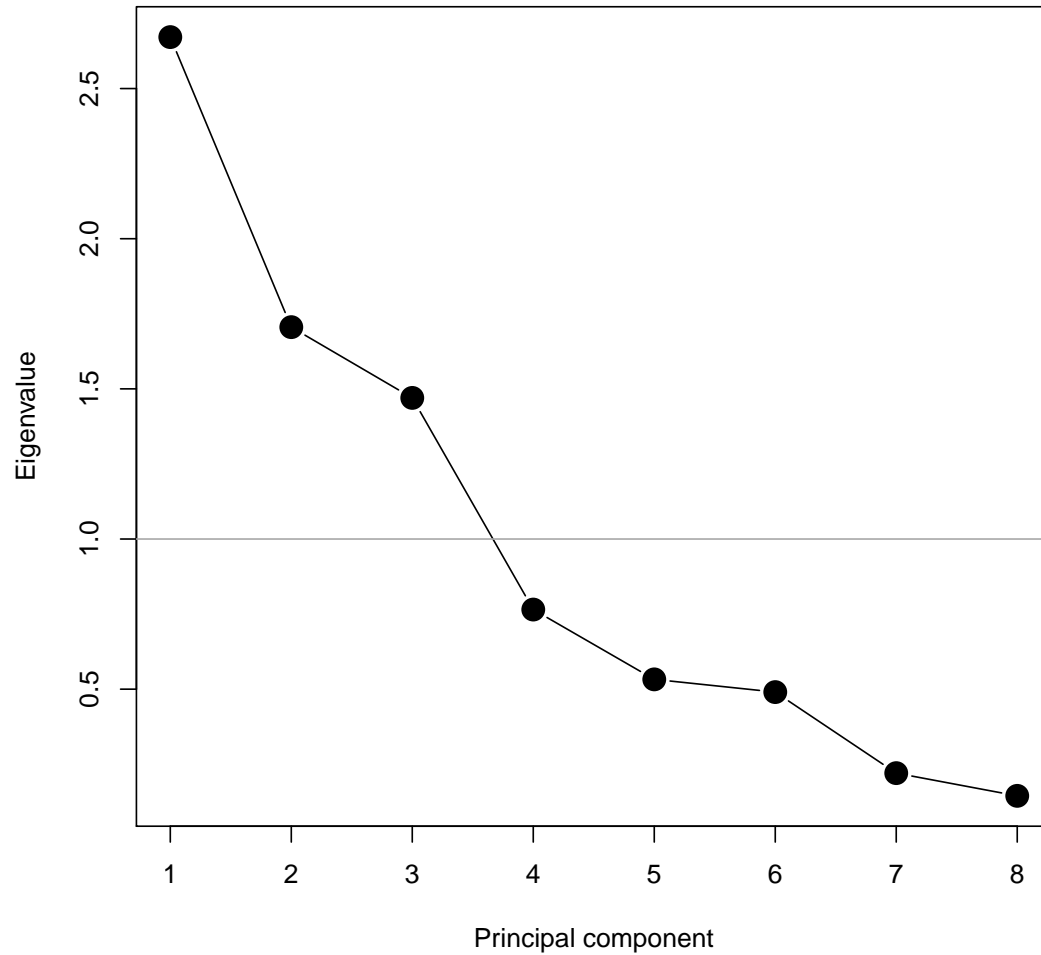


Figure A3: Results of parallel analysis conducted using the R package ‘paran’ (Dinno, 2018). Components with eigenvalues greater than 1 are retained.

819 Re-analysis with SEV-LTER data

820 To further explore the consequences of relying on down-scaled climate data, we
 821 re-ran our demographic analysis using the SEV-LTER meteorological data and

822 compared the results to those based on ClimateWNA. First, we conducted PCA on
 823 raw seasonal temperature and precipitation values from SEV Meteorological Sta-
 824 tion 50 over the observation years 2004–2017. As in our analysis of ClimateWNA
 825 data, parallel analysis supported retention of three principal components. Vari-
 826 able loadings onto these PCs are shown in Fig. A4 and show a pattern similar to
 827 ClimateWNA data whereby PC1 was dominated by annual differences (cool- and
 828 warm-season variables loaded similarly) and PC2-3 were dominated by seasonal
 829 climate factors. Second, we fit the full set of vital rate models to these three PCs
 830 and used stochastic variable selection (Appendix B) to eliminate weakly supported
 831 climate covariates. We then re-fit the vital rate models including variables with
 832 $\hat{z}_i > 0.1$ (see Appendix B). These fitted models are shown in Fig. A5.

833 We compared results based on the two data sources in several ways. First,
 834 we compared the inter-annual variances associated with year random effects in
 835 the statistical models. We found that, for survival in particular, random variance
 836 across years was much lower using SEV-LTER data as climate covariates com-
 837 pared to ClimateWNA (Fig. A6). This tells us that, as expected, on-site data
 838 provided greater resolution of climate drivers, since less inter-annual variation in
 839 survival was attributed to process error. Second, we used the IPM derived from
 840 each data source to generate two predicted time series of λ during the study years.
 841 We found that SEV-LTER climate PCs explained 78% of inter-annual variation
 842 in λ , an improvement over the 60% explained by ClimateWNA PCs. Finally, the
 843 year-by-year estimates were significantly correlated between the two data sources
 844 (Fig. A7A; Pearson's $r = 0.59$, $t_{10} = 2.34$, $P < 0.04$). When we additionally incor-
 845 porated year-specific random effects estimated from the statistical models, λ esti-
 846 mates were nearly perfectly correlated (Fig. A7B; Pearson's $r = 0.99$, $t_{10} = 40.36$,

847 $P < 0.0001$), as expected. This tells us that our qualitative conclusions based on
 848 the longer ClimateWNA time series of climate covariates is likely robust to the
 849 uncertainties introduced by downscaled data. However, the 18% loss of resolution
 850 with ClimateWNA tells us that using downscaled data inflated the contribution
 851 of process error to our back-casted estimates (Fig. C3A).

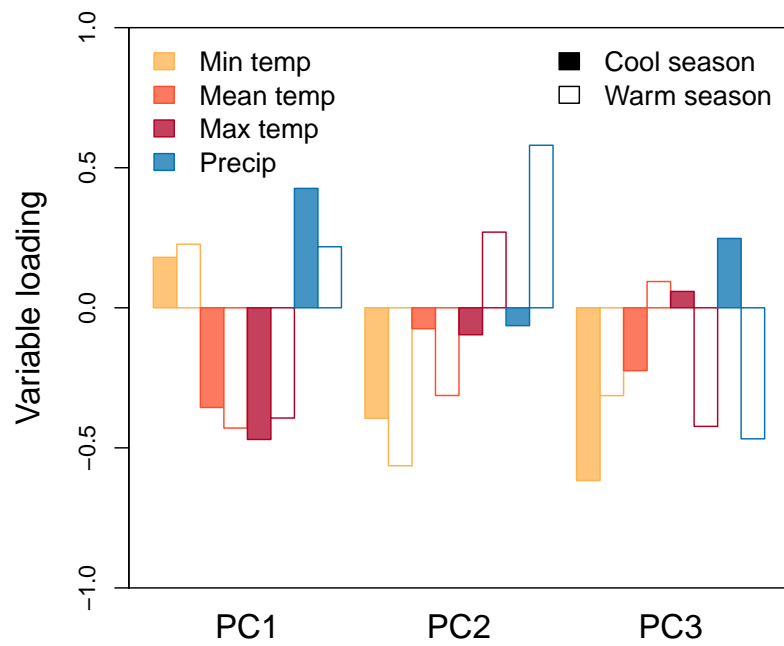


Figure A4: Principal components analysis of SEV-LTER meteorological data. Bars show loadings of raw variables onto three principal components. Layout as in Fig. 1.

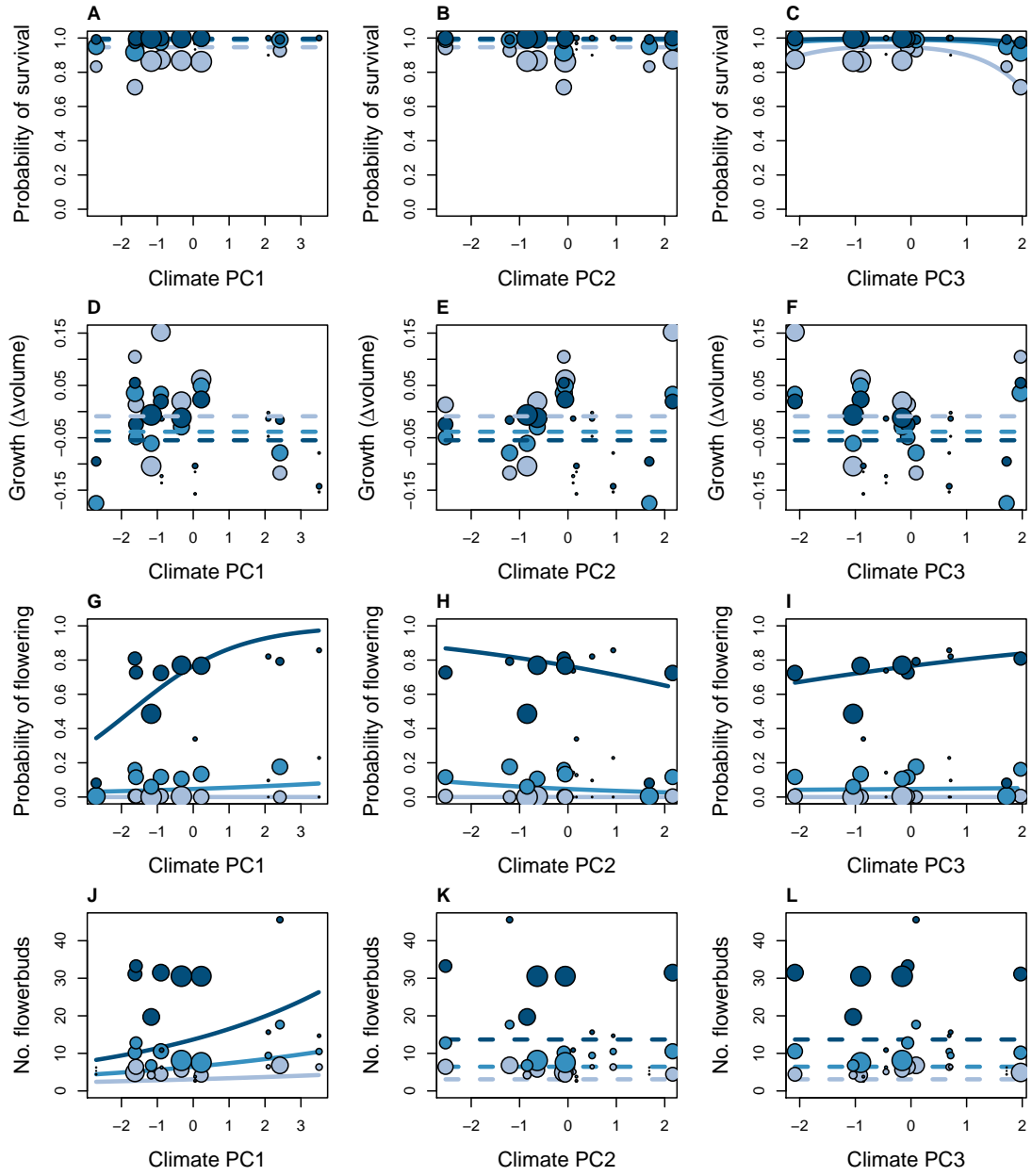


Figure A5: Vital rate data and fitted models using principal components of SEV-LTER meteorological data as climate covariates. Layout as in Fig. 2.

Climate PC	Model term	Survival	Growth	Flowering	Fertility
	Size	1	0.01	1	1
1	PC	0.06	0.01	0.07	0.07
1	PC*PC	0.03	0.01	0.05	0.01
1	PC*size	0.06	0.01	1	0.31
2	PC	0.06	0.01	0.13	0.05
2	PC*PC	0.03	0.01	0.05	0.03
2	PC*size	0.02	0.01	0.04	0.03
3	PC	0.78	0.02	0.09	0.04
3	PC*PC	0.88	0.02	0.08	0.03
3	PC*size	0.04	0.01	0.17	0.02

Table A2: Stochastic variable selection results based on climate data from SEV-LTER. Values (z) can be interpreted as the probability that a model coefficient is non-zero. Bolded values indicate terms retained in the final model.

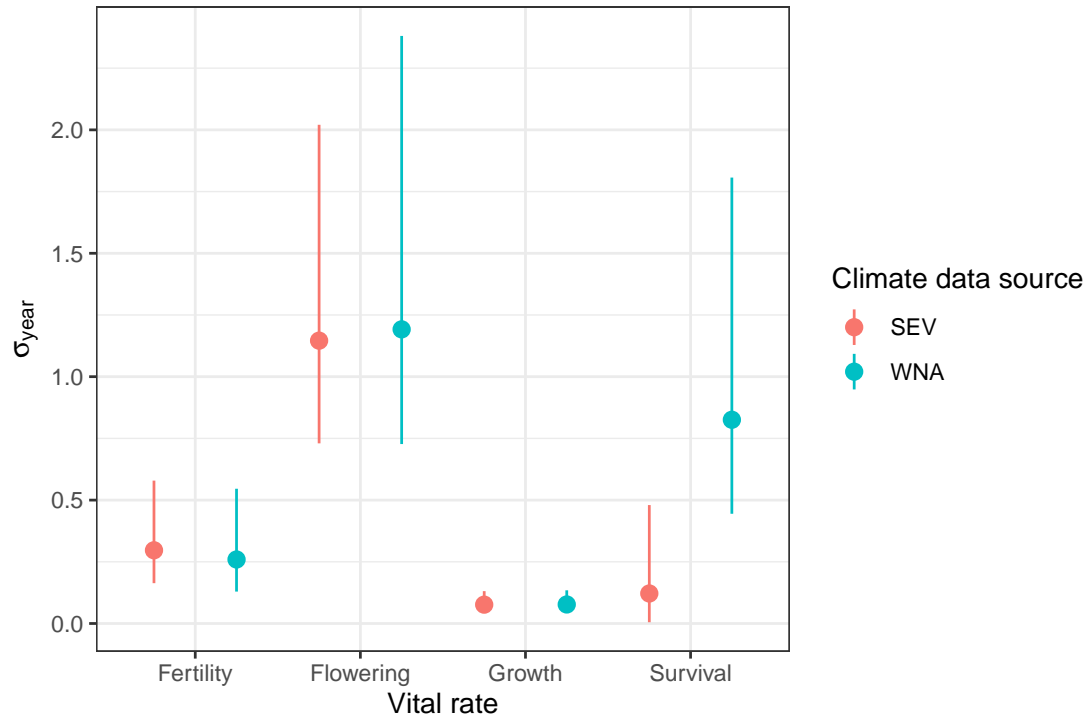


Figure A6: Posterior distributions of inter-annual variance (σ_{year}) associated with year random effects from vital rate models fit with two climate data sources (colors): ClimateWNA and SEV-LTER. Points show posterior means and bars show 95% credible intervals.

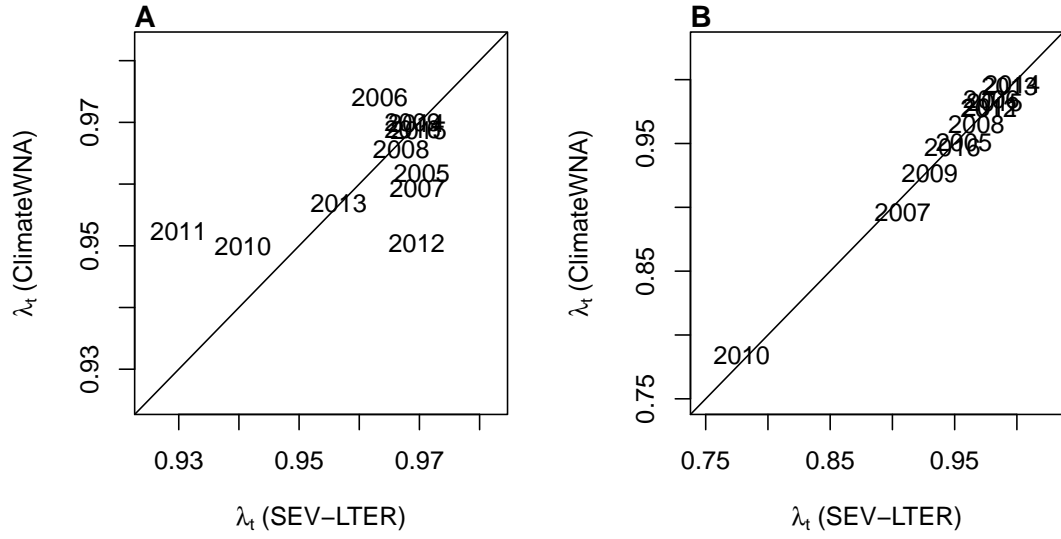


Figure A7: Comparison of year-specific estimates of λ from IPMs using either SEV-LTER (x -axis) or ClimateWNA (y -axis) as climate data sources. Diagonal lines show $y = x$. **A**, λ estimates based only on climate PCs (Pearson's $r = 0.59$, $t_{10} = 2.34$, $P < 0.04$); **B**, λ estimates based on climate and year random effects, which account for inter-annual differences not explained by the climate PCs (Pearson's $r = 0.99$, $t_{10} = 40.36$, $P < 0.0001$).

852 Appendix B: Stochastic variable selection

853 Because we intended to extrapolate the vital rate models into past climate environ-
854 ments that were not well represented during the long-term study, it was important
855 that we simplify the vital rate models to exclude unnecessary coefficients (which,
856 even if small in absolute value, could generate unrealistic predictions when ex-
857 trapolated over a greater range of climate than the models were fitted to). To
858 do this, we used stochastic variable selection, a ‘model-based model selection’
859 approach (Hooten & Hobbs, 2015) that generates weightings for each fixed-effect
860 coefficient, indicating the probability that the coefficient is non-zero. We employed
861 an approach based on George and McCulloch (1993) where each coefficient (C_i)
862 is modeled as a mixture distribution with zero and non-zero modes, where modal
863 frequency is determined by an indicator variable (z_i). The coefficient prior was:

$$C_i \sim (1 - z_i) * N(0, 0.1) + z_i * N(0, 1000) \quad (\text{B1})$$

$$z_i \sim \text{Bernoulli}(0.5) \quad (\text{B2})$$

864 The first term of the mixture distribution assigns, with probability $(1 - z_i)$, a
865 prior with mean zero and arbitrarily small variance, effectively forcing the poste-
866 rior estimate to equal zero. The second term assigns, with probability z_i , a prior
867 with mean zero and arbitrarily large variance, which allows for a non-zero pos-
868 terior estimate. The posterior distribution of the indicator variable z_i gives the
869 probability that the coefficient is non-zero. We estimated this probability for each
870 coefficient in Eq. B1 and retained in the final model all coefficients with a posterior

mean $\hat{z}_i > 0.1$, meaning that the model term is determined to be non-zero with 90% confidence. All z_i values from the full model are shown in Table B1.

Climate PC	Model term	Survival	Growth	Flowering	Fertility
	Size	1	0.53	1	1
1	PC	0.13	0.04	0.12	0.05
1	PC*PC	0.03	0.01	0.03	0.01
1	PC*size	0.06	0.01	0.08	0.07
2	PC	0.18	0.03	0.11	0.14
2	PC*PC	0.06	0.01	0.06	0.03
2	PC*size	0.04	0.02	1	0.27
3	PC	0.18	0.02	0.12	0.18
3	PC*PC	0.09	0.01	0.09	0.06
3	PC*size	0.06	0.01	0.13	0.03

Table B1: Stochastic variable selection results. Values (z) can be interpreted as the probability that a model coefficient is non-zero. Bolded values indicate terms retained in the final model.

873 Appendix C: Additional demographic modeling meth- 874 ods and results

875 We estimated a time series for the stochastic population growth rate (λ_S) over
876 the period 1900-2017 using a moving window approach. While the determinis-
877 tic growth rate for each year estimates the long-run growth rate expected if the
878 conditions of that year remained constant, the stochastic growth rate integrated
879 over a broader range of conditions, incorporating year-to-year fluctuations and
880 auto-correlation of climate variables.

We simulated population dynamics according to Equations 4–2 to estimate the stochastic population growth rate λ_S . We estimated λ_S for 10-year windows spanning the time series 1901–2017, such that the value of λ_S for year t reflects the stochastic growth rate for a climate environment defined by years t through $t + 9$. For each 10-year window, we simulated 1000 years of population dynamics, each year randomly drawing one of the 10 climate-years. For each year of the simulation, we calculated total population size as:

$$N_t = \int n(x)_t dx + B_{1,t} + B_{2,t} \quad (\text{C1})$$

and estimated the stochastic growth rate for that window as the expected value of the one-year growth rate:

$$\log(\lambda_S) = \mathbb{E}[\log(\frac{N_{t+1}}{N_t})] \quad (\text{C2})$$

Table C1: Parameter values of tree cholla IPM.

Parameter description	Symbol	Mean	95%CI
Survival coefficients	β_0	3.33	(1.4 – 5.25)
	β_1	1.31	(1.18 – 1.44)
	ρ_1^1	-0.11	(-0.82 – 0.61)
	ρ_1^2	0.41	(-0.25 – 1.13)
	ρ_1^3	-0.28	(-0.84 – 0.3)
Survival year variance	σ_{year}	0.9	(0.44 – 1.81)
Growth coefficients	β_0	-0.03	(-0.08 – 0.02)
	β_1	-0.02	(-0.03 – -0.02)
Growth residual variance	σ	0.25	(0.25 – 0.26)
Growth year variance	σ_{year}	0.08	(0.05 – 0.13)
Flowering coefficients	β_0	-4.76	(-7.37 – -2.22)
	β_1	5.17	(4.78 – 5.54)
	ρ_1^1	-0.26	(-1.27 – 0.7)
	ρ_1^2	0.07	(-0.85 – 1.01)
	ρ_3^2	1.11	(0.65 – 1.61)
	ρ_1^3	-0.04	(-0.79 – 0.77)
	ρ_3^3	0.21	(-0.06 – 0.47)
Flowering year variance	σ_{year}	1.28	(0.73 – 2.38)
Fertility coefficients	β_0	-0.25	(-0.6 – 0.1)
	β_1	2.22	(2.01 – 2.42)
	ρ_1^2	0.06	(-0.15 – 0.28)
	ρ_3^2	0.17	(-0.01 – 0.35)
	ρ_1^3	0.12	(-0.04 – 0.29)
Fertility year variance	σ_{year}	0.28	(0.13 – 0.55)
Seeds per fruit	κ	113.46	(93.47 – 132.59)
Recruitment into seed bank	δ	0.03	(0.02 – 0.05)
Germination rates	γ_1	0.0059	(0.0047 – 0.0073)
	γ_2	0.0044	(0.0033 – 0.0056)
Seedling size distribution	μ_s	-3.49	(-3.62 – -3.37)
	σ_s	0.23	(0.15 – 0.35)
Seedling survival	ω	0.5	(0.002 – 0.998)
Size bounds	L	-3.94	
	U	1.89	

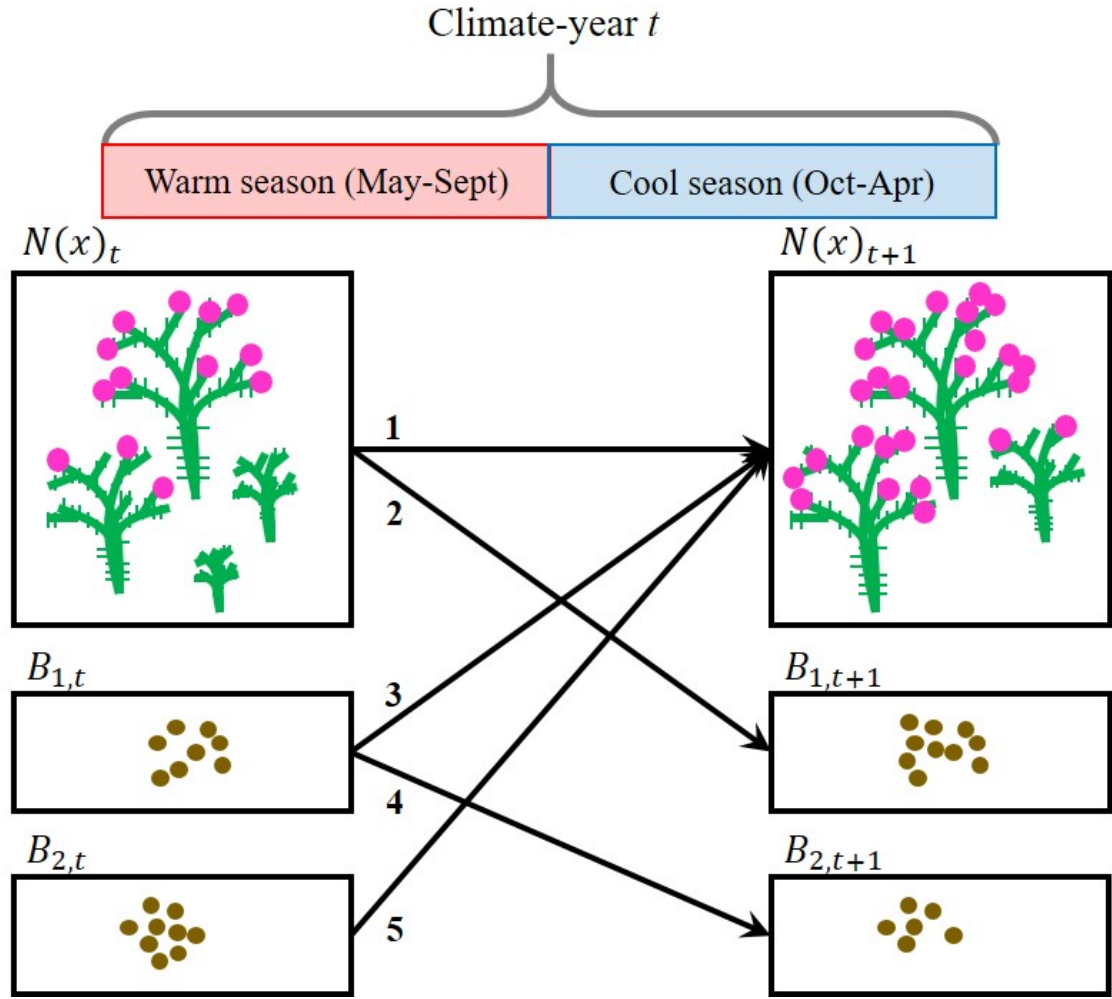


Figure C1: *C. imbricata* life cycle and census timing with respect to warm- and cool-season climate. Numbered arrows correspond to demographic events that occur during a transition year: (1) established plants survive and grow, (2) plants that are reproductive in year t contribute seeds that will make up the 1-yo seed bank in year $t+1$, (3) a fraction of seeds in the 1-yo seed bank survive and recruit into the plant population as seedlings in year $t+1$, (4) another fraction of seeds in the 1-yo seed bank survives and remains to form the 2-yo seed bank in year $t+1$, (5) a fraction of seeds in the 2-yo seed bank survive and recruit into the plant population as seedlings in year $t+1$. Survival and growth from year t to year $t+1$ (arrow 1) depended on climate year year t , whereas flowering and flowerbud production in year t (components of arrow 2) depended on climate in year $t-1$.

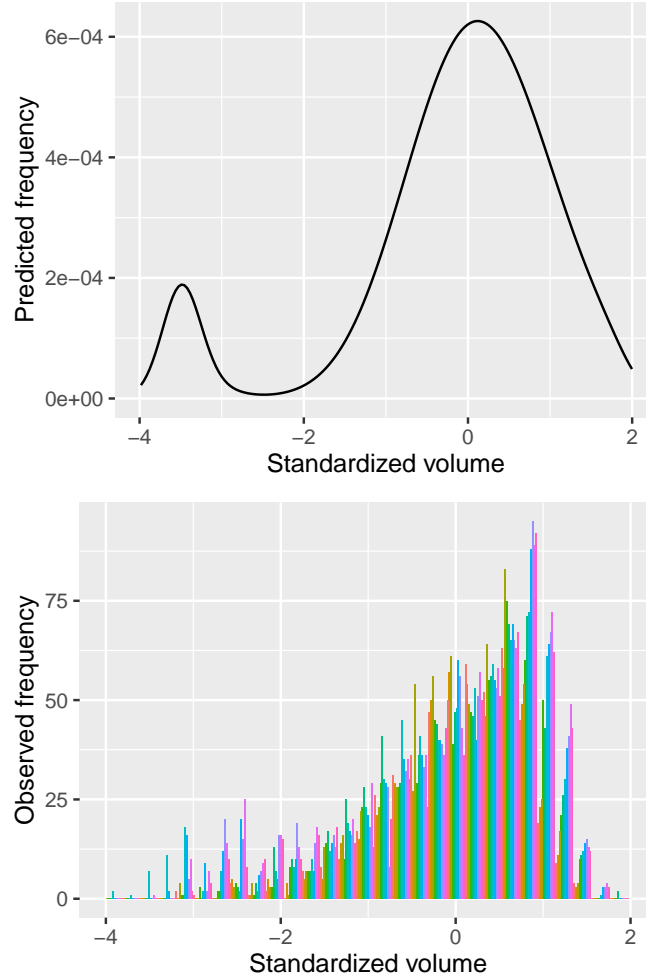


Figure C2: Comparison of predicted (top) and observed (bottom) size distributions, where size was the natural logarithm of plant volume standardized to mean zero. In the bottom panel, different colors represent different years. The predicted stable size distribution (evaluated at the average climate) corresponded well to the observed size distribution, though very large plants were over-represented in the observed distribution. This is consistent with the idea that the population may have recently transitioned into decline, whereby the persistence of large plants may reflect a legacy of positive growth rates. Also, the peak for new recruits was at a larger size in the observed distribution, but this was likely a consequence of the fact that we rarely detected new recruits. The “new” plants in our plots each year were likely several years old.

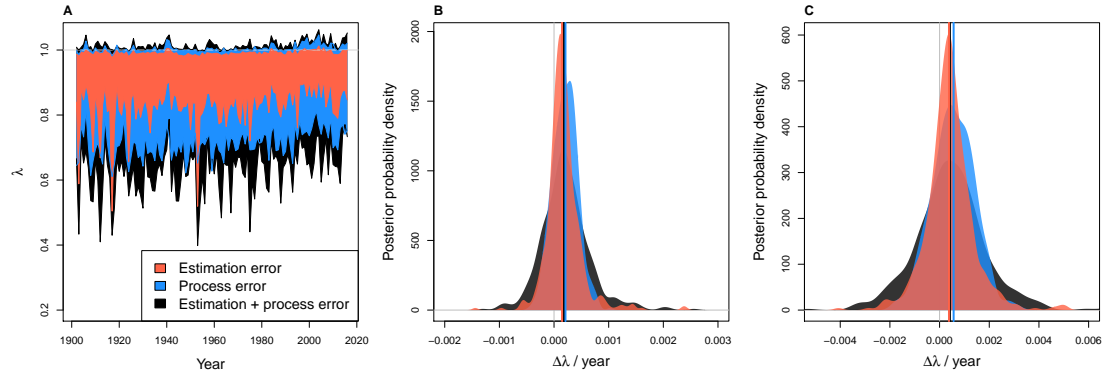


Figure C3: **A**, Time series of back-casted asymptotic population growth rates (λ) predicted based on inter-annual variation in three climate PCs. Shaded regions show the 95% credible interval of the posterior probability distributions for three uncertainty scenarios: estimation error only (parameter uncertainty; red), process error only (year-to-year heterogeneity unrelated to the climate PCs; blue), and both estimation and process error (black). **B**, **C**, Posterior probability distribution for the change in λ per year based on the entire time series (**B**) or years since 1970 (**C**). Vertical lines show the medians of the posterior distributions. Colors as in **A**.

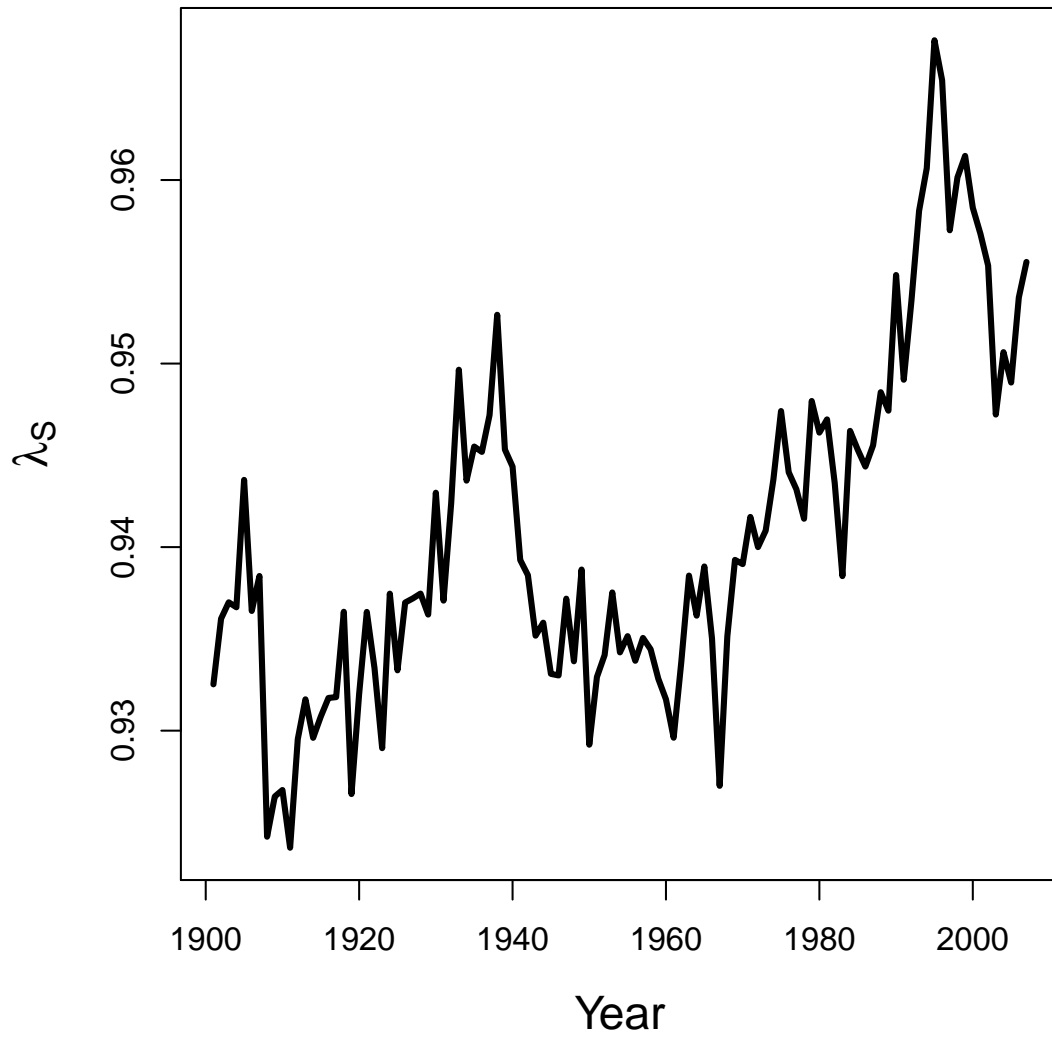


Figure C4: Time series of stochastic population growth rates (λ_S). Values are based on a 10-year sliding window such that λ_S is year t is based on the climate regime over the years t through $t + 9$

881 Appendix D: Exploring the consequences of climate 882 extrapolation

883 Our analysis in the main text relied on extrapolating demographic responses to
884 climate into climate environments that were not directly observed during our field
885 study. For example, high values of PC1 and low values of PC2 were under-
886 represented during the study years (Fig. D1). We explored the consequences
887 of this extrapolation by re-running our demographic analysis with bounds on cli-
888 mate responses. For each vital rate that responded to a climate PC according to
889 some function $f(PC)$, we defined a second function $f^*(PC)$ as:

$$f^*(PC) = \begin{cases} f(PC_L), & \text{if } PC < PC_L \\ f(PC_U), & \text{if } PC > PC_U \\ f(PC), & \text{otherwise} \end{cases} \quad (\text{D1})$$

890 where PC_L and PC_U are the lower and upper bounds, respectively, of the observed
891 range of PC values. For simulations into historical climates more extreme than
892 observed, this approach pins demographic responses to equal the responses at
893 observed extrema, as can be seen in λ responses to PC variation (Fig. D2). We
894 repeated our back-casting analysis using this approach.

895 Results show that our qualitative results are not affected by climate extrapola-
896 tion. The back-casted time series of λ was generally consistent with and without
897 extrapolation (Fig. D3). The main differences were in the extreme low λ values,
898 which were lower with extrapolation. Both time series yielded a positive temporal
899 trend, though the mean change in λ per year was 35% weaker for the entire time

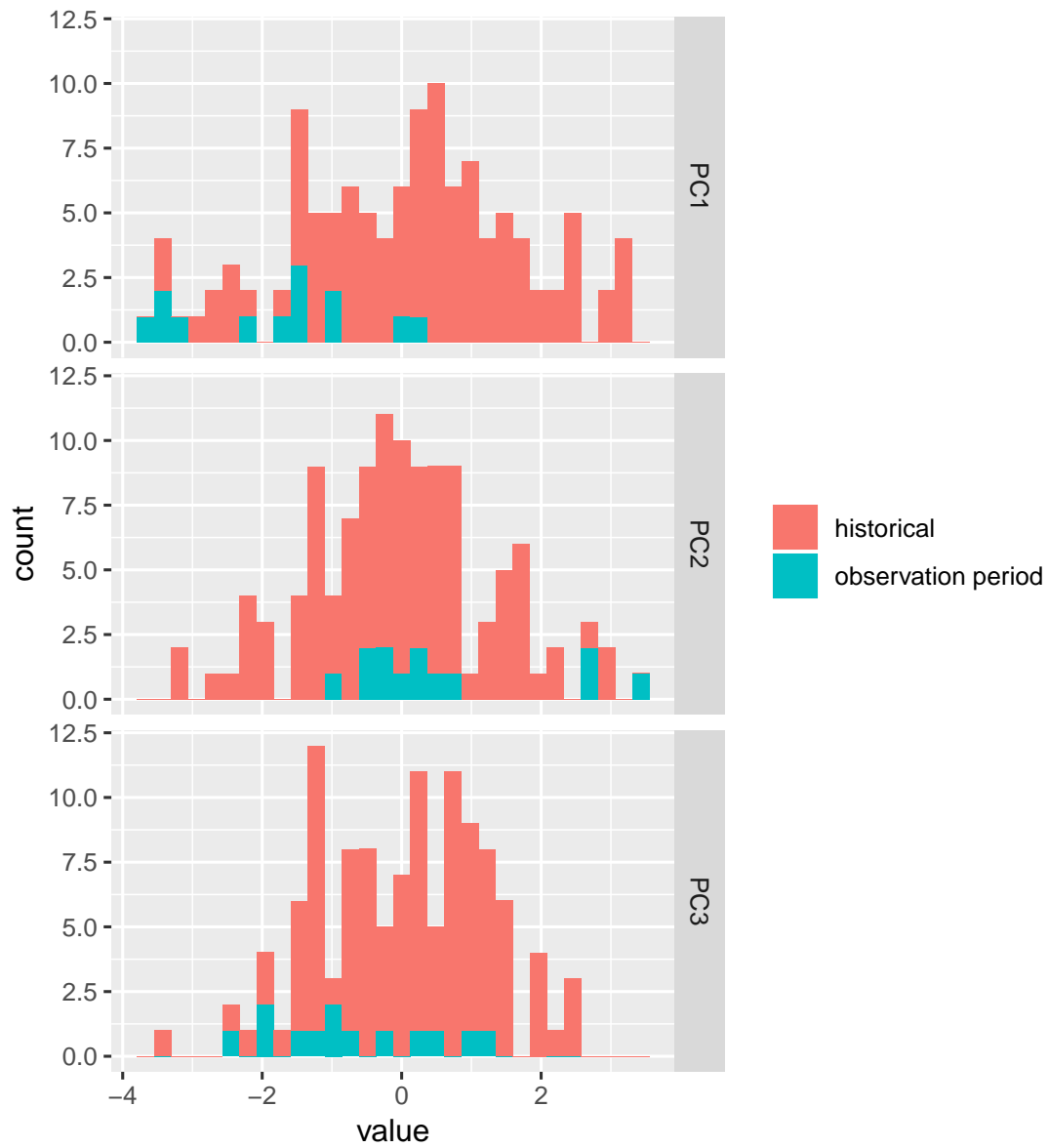


Figure D1: Distributions of observed climate values during the observation period (2004–2017) relative to historical values (1901–2016). Climate values are three principal components of inter-annual variation in cool- and warm-season temperature and precipitation.

series and 26% weaker since 1970 when vital rates were not extrapolated (Fig. D2). The limited influence of extrapolation was due to the fact that we relied

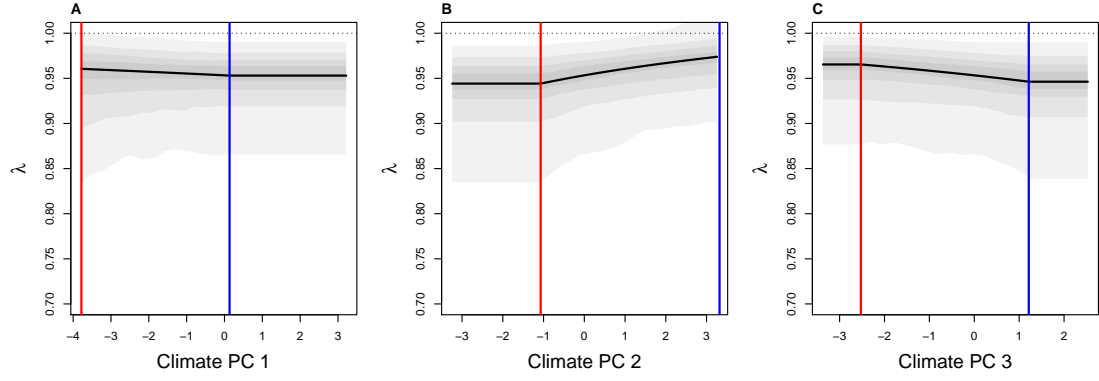


Figure D2: Relationships between λ and three climate PCs with no extrapolation into unobserved climate conditions. For PC values lower than the minimum (red vertical lines) and greater than the maximum (blue vertical lines) of the observation period, demographic responses were forced to match the extrema of the observation period according to Eq. D1.

902 most heavily on extrapolation for PC1 (Fig. D1). As we show in the main paper,
 903 this PC has changed the most during the historical record but it had the weakest
 904 effects on cactus demography.

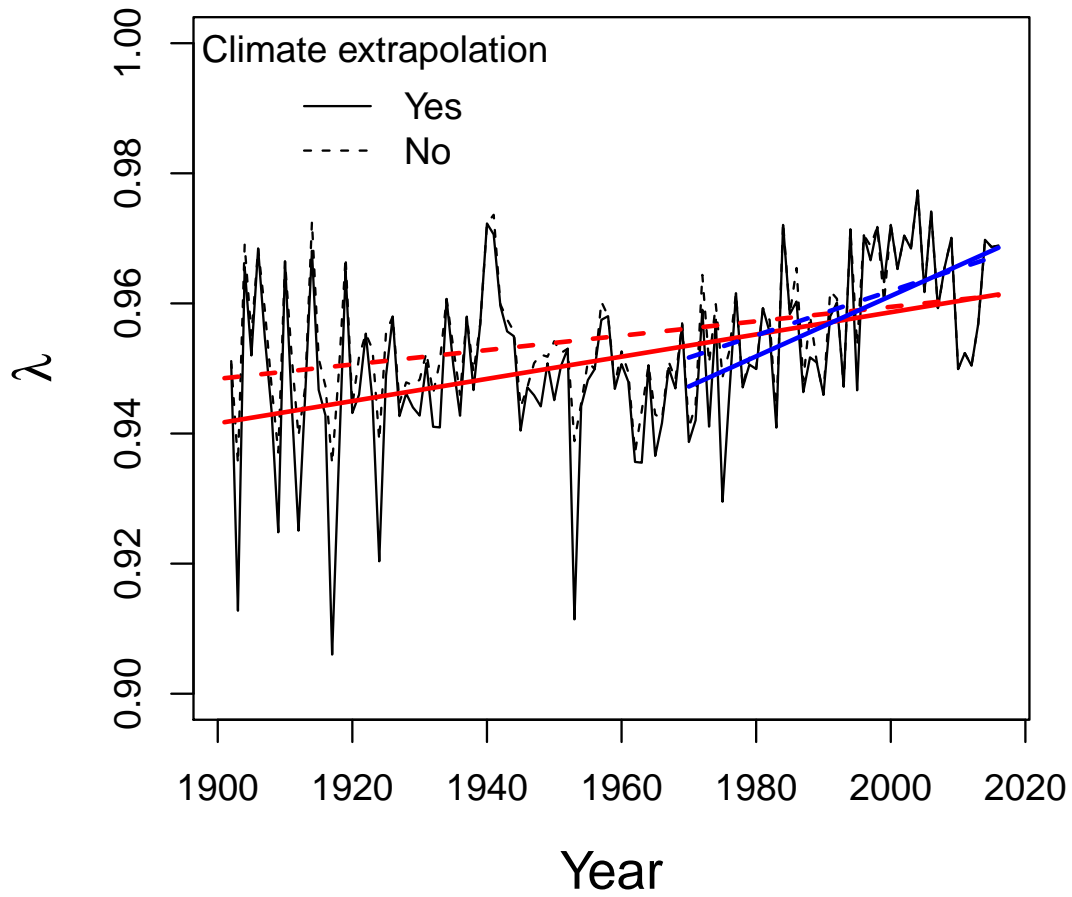


Figure D3: Back-casted values of climate-dependent population growth (λ) with (solid lines) and without (dashed lines) extrapolation of vital rate responses to unobserved climate conditions based on posterior mean parameter values. Red and blue lines show fitted regressions for the entire time series and since 1970, respectively.